Pore-forming toxins: ancient, but never really out of fashion

Matteo Dal Peraro[1] and F. Gisou van der Goot[2]

Abstract | Pore-forming toxins (PFTs) are virulence factors produced by many pathogenic bacteria and have long fascinated structural biologists, microbiologists and immunologists. Interestingly, pore-forming proteins with remarkably similar structures to PFTs are found in vertebrates and constitute part of their immune system. Recently, structural studies of several PFTs have provided important mechanistic insights into the metamorphosis of PFTs from soluble inactive monomers to cytolytic transmembrane assemblies. In this Review, we discuss the diverse pore architectures and membrane insertion mechanisms that have been revealed by these studies, and we consider how these features contribute to binding specificity for different membrane targets. Finally, we explore the potential of these structural insights to enable the development of novel therapeutic strategies that would prevent both the establishment of bacterial resistance and an excessive immune response.

Pore-forming toxins (PFTs) are produced by many pathogenic bacteria and are important components of their virulence arsenal[1]. PFTs are the largest class of bacterial toxins and constitute a major class of pore-forming proteins (PFPs) — an ancient protein family also found in non-pathogenic bacteria and indeed in all kingdoms of life. Although PFTs were initially viewed as unsophisticated proteins that simply form pores in membranes, advances in the past decade have revealed, with great detail, the astonishing complexity of their architecture and dynamics[2]. During bacterial infection, through the disruption of epithelial barriers and interactions with the immune system, PFTs promote pathogen growth and dissemination, although their precise contribution to these processes is difficult to establish. As with other PFPs, PFTs alter the plasma membrane permeability of their targets cells, potentially leading to cell death, but may also lead to a more subtle manipulation of cellular functions[1–3] (BOX 1).

PFTs (and, more generally, PFPs) can be classified into two large groups — α-PFTs and β-PFTs — based on whether the secondary structure of their membrane-spanning elements is composed of α-helices or β-barrels, respectively[4–6]. All PFPs initially fold into a water-soluble, generally monomeric, structure (FIG. 1). In the past decade, many structures of PFTs and PFPs have been described, which have revealed an elaborate range of strategies used by these proteins to undergo the very unusual metamorphosis from a soluble protein to a transmembrane protein. Six families have now been identified: three families of α-PFTs and three families of β-PFTs (TABLE 1).

In all documented cases, PFPs recognize the target cell by binding to specific receptors, which can be sugars, lipids or proteins. Surface binding leads to a drastic increase in the local concentration of PFPs, largely owing to a reduction in the dimensions of protein diffusion from a three-dimensional space to a two-dimensional plane. This increase in concentration favours oligomerization, which is a step required for pore formation for all classes of PFPs. Oligomerization either precedes or is concomitant to the exposure of hydrophobic surfaces that leads to membrane insertion (FIG. 1). The primary focus of this Review is PFTs, which are mainly — but not exclusively — found in bacteria; however, it should be noted that PFPs with similar structures are increasingly being found in eukaryotes, in particular as components of the immune systems of animals[7–9].

Detailed analyses have revealed that different PFTs form pores with distinctive properties, which in turn induce different phenotypes and responses in target cells[2]. Although perforation of the plasma membrane by PFTs always leads to an increase in membrane permeability, the molecules to which the membrane becomes permeable can vary. Depending on the toxin, the pore may only allow specific ions, such as potassium and/or calcium, to pass through; in other cases, it may be permeable to small molecules such as ATP, or larger molecules such as proteins (BOX 1). Therefore, an in-depth characterization of pore architecture is required to fully understand the cellular response to a specific PFT. Furthermore, the PFT concentration differs according to body site during infection. The most extreme cellular

[1]*Institute of Bioengineering, School of Life Sciences, Ecole Polytechnique Fédérale de Lausanne (EPFL), 1015 Lausanne, Switzerland.*
[2]*Global Health Institute, School of Life Sciences, Ecole Polytechnique Fédérale de Lausanne (EPFL), 1015 Lausanne, Switzerland.*
Correspondence to M.D.P. and F.G.v.d.G.
matteo.dalperaro@epfl.ch; gisou.vandergoot@epfl.ch

doi:10.1038/nrmicro.2015.3
Published online 7 Dec 2015

Box 1 | **Cellular responses to pore formation**

The mechanism and amplitude of the membrane permeabilization that results from pore formation by pore-forming toxins (PFTs) depends on the identity of the PFT and its concentration in the vicinity of the target cell. These differences in turn lead to a large diversity in the cellular responses to PFTs and in the potential mechanisms by which the membrane might be repaired. These responses have recently been reviewed elsewhere[2], but here we briefly discuss the cellular response to changes in ion concentrations and the mechanisms of membrane repair that are induced in response to membrane damage.

Impact on ion concentration. Pore formation caused by most PFTs leads to a drop in cellular potassium concentration that is sensed through mechanisms that are not yet elucidated. Cells respond by activating several signalling pathways, including the inflammasome complex, mitogen-activated protein kinase (MAPK) pathways (such as the p38 and the extracellular signal-regulated kinase (ERK) pathways) and autophagy[168]. Activation of the inflammasome complex further results in the downstream activation of caspase 1 and, subsequently, cleavage of interleukin-1β (IL-1β) and possibly other targets. Inflammasome activation has been reported for various toxins, including aerolysin[169], *Vibrio cholerae* cytolysin (VCC)[170], clostridium β-toxin[171] and *Staphylococcus aureus* PFTs[172–174]. Activation of MAPKs[1], as well as autophagy, was found for several PFTs, with recent examples including *Serratia marcescens* ShlA[175] and *S. aureus* α-haemolysin (Hla)[176,177]. Finally, the decrease in cellular potassium was also found to trigger the formation of lipid droplets[168], dephosphorylation of histones[178] and the arrest of protein synthesis[168]. This latter event, combined with autophagy, enables cells to adopt a low-energy consumption mode that might allow survival until membrane repair.

Many PFTs also permeabilize the plasma membrane to calcium. As calcium is a potent second messenger, the resulting increase in the concentration of intracellular calcium triggers the activation of various signalling cascades, such as the release of calcium from intracellular stores and the activation of calpain and other proteolytic cascades[2].

Membrane repair. The ability of cells to restore plasma membrane integrity following damage caused by PFTs, and the speed with which this occurs, varies between cell types and depends on the identity of the toxin and its concentration[2]. Furthermore, membrane repair following damage by cholesterol-dependent cytolysins (CDCs) is highly dependent on the entry of calcium[179–181]. Three main mechanisms of membrane repair have been proposed. The first is disassembly of the pore-forming complex, although there is currently no real evidence for this and it is unlikely for pores such as those formed by aerolysin, the stability of which is remarkable[182]. The second is uptake of the pores by endocytosis, with the aim of degrading the pores in lysosomes[183] or secreting them into the extracellular space via exosomes[184]. Repair by endocytosis has been proposed for streptolysin O (SLO)[183] and may involve the uptake of caveolae[185]. The third proposed mechanism is shedding of PFT-containing membrane patches through the formation of extracellular vesicles, which has also been proposed for SLO[186]. It was recently shown that the endosomal sorting complex required for transport (ESCRT) machinery was required for membrane repair following mechanical damage or damage caused by PFTs[187]. This machinery is classically involved in the biogenesis of intraluminal vesicles of multivesicular bodies[188], but has also been shown to be involved in viral budding[189,190], consistent with the fact that both events require budding of the membrane away from the cytosol. These recent findings would thus be consistent with membrane repair through the budding of extracellular vesicles.

Lipid droplets
Cellular organelles that store metabolic energy in the form of neutral lipids, such as triglycerides. These neutral lipids form the core of the droplet, which is surrounded by a phospholipid monolayer.

Exosomes
Vesicles that are released into the extracellular space from the lumen of multivesicular bodies.

response possible is cell death, by necrosis, programmed necrosis, pyroptosis or apoptosis[2]; however, even at sublytic concentrations, PFTs remain toxic as they can still modify cellular behaviour. Through these various effects, PFTs contribute to bacterial growth and colonization, in part by protecting the invading bacteria from the host immune response[10,11].

In this Review, we discuss recent work that has revealed the pore architectures and mechanisms of pore formation for each family of PFTs. Furthermore, we show how modularity of receptor recognition enables different PFTs within the same family to target different cell types and we consider how elucidating the mechanism of pore formation at an atomic level (BOX 2) may eventually lead to the development of new therapeutic strategies to fight infection by targeting virulence rather than bacterial survival.

α-PFTs

The colicin family. Pore-forming colicins are produced by *Escherichia coli* to kill related bacterial species by forming pores in the inner bacterial membrane[12]. They have a crucial role in shaping the microbial population, possibly by killing competitors or invading an occupied niche[13].

Before the first structures of colicins were solved, bioinformatics analyses indicated that colicins were likely to contain hydrophobic α-helices, in common with many other transmembrane proteins. The first PFT structure to be solved was that of the pore-forming domain of colicin A, which revealed an 'inside-out membrane protein' fold (that is, a hydrophobic helical hairpin sheltered within a bundle of amphipathic α-helices) that was consistent with a protein that can switch between soluble and transmembrane conformations[14] (FIG. 2a).

Pore formation by colicins minimally requires the insertion of the hydrophobic helical hairpin into the inner membrane, which produces a nonspecific voltage-gated channel[15,16]; this leads to membrane depolarization, ATP depletion and, ultimately, target cell death[13]. The exact structure and stoichiometry of these pores has remained a mystery, owing to their inability to form stable oligomeric complexes that are amenable to structural analysis[5]. It is generally accepted that, upon interaction with the target membrane, the amphipathic helices move away from the hydrophobic helical hairpin, enabling its insertion into the membrane[16]. This rearrangement leads to the formation of a structure known as the 'umbrella' structure, a model originally proposed for colicin A[17,18] (FIG. 2a) but subsequently extended to colicin E1 and colicin Ia[19–22], and more recently supported by electron paramagnetic resonance (EPR) measurements on spin-labelled colicin A[23]. However, the formation of this structure seems to be insufficient for channel formation; therefore, it is expected that other mechanisms operate in concert with umbrella formation. One possibility is that the electrostatic complementarity of colicins and negatively charged bacterial membranes promotes the insertion of some of the other amphipathic helices into the membrane[12,24]. Another possibility is that the insertion of the hydrophobic hairpin could trigger multimerization, as observed for colicin A[25] (that is, dimers) and colicin Ia[26] (that is, trimers of dimers) (TABLE 1).

Outside of the colicin family, the colicin fold has subsequently been found in the translocation domain of diphtheria toxin[27], which translocates the catalytic subunit of the toxin across endosomal membranes. The pore-forming insecticidal Cry toxins produced by *Bacillus thuringiensis*[28] also have a colicin fold, and a homologous fold of probable common ancestry with colicins is present in the membrane translocators that form the tip of bacterial type III secretion systems[29]. Quite remarkably, eukaryotic proteins of the BAX and BCL-2 homologous antagonist/killer (BAK) family — which are thought to originate from

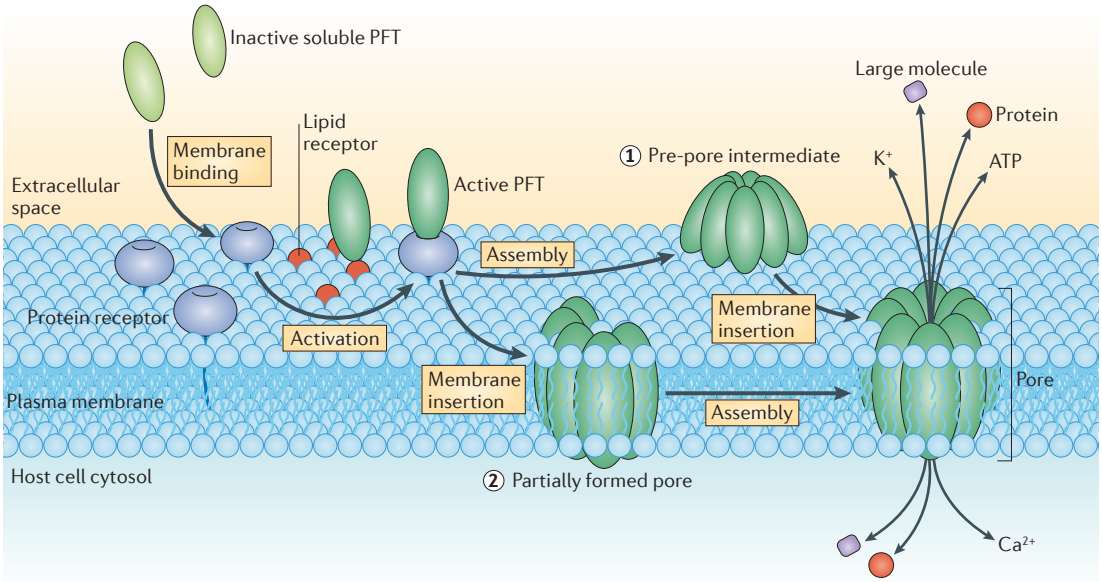

Figure 1 | **Molecular mechanisms of pore formation.** Schematic representation of the pore formation pathway of pore-forming toxins (PFTs). Soluble PFTs are recruited to the host membrane by protein receptors and/or specific interactions with lipids (for example, sphingomyelin for actinoporins or sterols for cholesterol-dependent cytolysins (CDCs)). Upon membrane binding, the toxins concentrate and start the oligomerization process, which usually follows one of two pathways. In the pathway followed by most β-PFTs, oligomerization occurs at the membrane surface, producing an intermediate structure known as a pre-pore (mechanism 1), which eventually undergoes conformational rearrangements that lead to concerted membrane insertion. In the pathway followed by most α-PFTs, PFT insertion into the membrane occurs concomitantly with a sequential oligomerization mechanism, which can lead to the formation of either a partially formed, but active, pore (mechanism 2), or the formation of complete pores. Although classified as β-PFTs, CDCs also share some of the features of this second pathway, as they can also form intermediate structures (known as 'arcs', named after their shape) during pore formation. In both α-PFT and β-PFT pathways, the final result is the formation of a transmembrane pore with different architecture, stoichiometry, size and conduction features, which promote the influx or efflux of ions, small molecules and proteins through the host membrane, and trigger various secondary responses involved in the repair of the host membrane. Note that, although the host membrane shown here is the eukaryotic plasma membrane, some PFTs are antibacterial and form pores in the inner membranes of Gram-negative bacteria or the cell membranes of Gram-positive bacteria.

Caveolae
Surface invaginations that may pinch off to allow cellular uptake of extracellular material.

Multivesicular bodies
Late endocytic organelles that contain intraluminal vesicles that are formed by inward invagination of the limiting membrane.

Programmed necrosis
A form of necrosis that is mediated by regulated pathways.

Pyroptosis
A caspase 1-dependent form of programmed cell death that occurs as an antimicrobial response.

Electron paramagnetic resonance
(EPR). A spectroscopy technique used to study paramagnetic molecules (that is, molecules with unpaired electrons). In biology, paramagnetic spin labels are covalently added to protein complexes to extract low-resolution information about their structure and dynamics.

phages — also have a colicin-like fold[30]. These proteins are involved in the control of apoptosis and serve to permeabilize mitochondria — that is, symbiotic prokaryotes[30,31], consistent with the ancestral role of colicins.

The ClyA family. The cytolysin A (ClyA) family of α-PFTs includes the following toxins: ClyA (also known as haemolysin E (HlyE)), which is produced by certain strains of *E. coli* and by *Salmonella enterica* and *Shigella flexneri*[32]; and the *Bacillus cereus* toxins non-haemolytic tripartite enterotoxin (Nhe; which, despite its name, is haemolytic)[32] and the B component of haemolysin BL enterotoxin (Hbl)[33] (TABLE 1). Although ClyA PFTs have been reported to be virulence factors, the organisms in which they have been found already produce several toxins and effectors, and thus the breadth of toxicity and identity of specific receptors of this family of PFTs is still an open field of investigation[34].

ClyA is one of the few PFTs for which the structure has been solved both in the soluble[35] and transmembrane[36] form, revealing the unique pore-formation process of this family of PFTs, which involves remarkable conformational changes. In solution, ClyA is an elongated, entirely α-helical protein, except for a short hydrophobic β-hairpin known as the β-tongue (FIG. 2a). In the vicinity of cholesterol-containing membranes, the β-tongue detaches from the core of the protein and dips into the lipid bilayer. This event triggers a massive rearrangement of the distal amino-terminal amphipathic α-helix, which swings around to reach the membrane. The length of this N-terminal helix varies between the members of this PFT family, as is apparent from the recently solved structure of NheA, a component of the ripartite Nhe toxin, in which the helix is much shorter[37]. This variation in length might have major consequences on the pore formation process and it has been proposed that NheA could even form β-barrel pores by a mechanism that has not yet been determined[37].

Subsequently, pore formation by ClyA requires circular oligomerization of the toxin by a sequential mechanism[38], which shares some common features with the actinoporins family (see below). This, in turn, concentrates the amphipathic helices in the centre of the ring-like structure, forming a helical barrel that inserts into the membrane by a wedge-like mechanism (FIG. 2a).

An alternative, contrasting pore formation process has been proposed whereby ClyA would oligomerize into soluble pre-pores encapsulated within bacterial

Table 1 | **Classification of PFT families***

PFT	Family	Class	Organisms	Stoichiometry	Receptor
Colicin E1	Colicins	α	*E. coli*	1–n	At IM/OM
Colicin Ia	Colicins	α	*E. coli*	1–n	At IM/OM
Colicin A	Colicins	α	*E. coli*	2	At IM/OM
Colicin N	Colicins	α	*E. coli*	2–6	IM/LPS-OM
Equinatoxin II (EqtII)	Actinoporins	α	*A. equina*	4	Sphingomyelin
Sticholysin II (StnII)	Actinoporins	α	*S. helianthus*	4	Sphingomyelin
Fragaceatoxin C (FraC)	Actinoporins	α	*A. fragacea*	8–9	Sphingomyelin
Cytolysin A (ClyA also known as HlyE)	ClyA	α	*E. coli*, *S. enterica*, *S. flexneri*	12	Cholesterol
Non-haemolytic tripartite enterotoxin (Nhe)	ClyA	α	*B. cereus*	-	Cholesterol
Haemolysin BL (Hbl)	ClyA	α	*B. cereus*	7–8	Cholesterol
α-haemolysin (Hla)	Haemolysins	β	*S. aureus*	7	PC/ADAM10/disintegrin
γ-haemolysin (Hlg)	Haemolysins	β	*S. aureus*	8	PC
Leukocidins (for example, HlgACB, LukED)	Haemolysins	β	*S. aureus*	8	CCR5, CXCR1, CXCR2, CCR2, C5aR C5L2,
Necrotic enteritis toxin B (NetB)	Haemolysins	β	*C. perfringens*	7	Cholesterol
δ-toxin	Haemolysins	β	*C. perfringens*	7	Monosialic ganglioside 2 (GM2)
V. cholerae cytolysin (VCC)	Haemolysins	β	*V. cholerae*	7	Glycoconjugates
V. vulnificus haemolysin (VVH)	Haemolysins	β	*V. vulnificus*	7	Glycerol, *N*-acetyl-D-galactosamine
Aerolysin	Aerolysin	β	*Aeromonas* spp.	7	GPI-anchored proteins (for example, CD52)
α-toxin	Aerolysin	β	*Clostridium* spp.	-	GPI-anchored proteins
Hydralysin	Aerolysin	β	*Cnidaria* spp.	-	-
ε-toxin	Aerolysin	β	*C. perfringens*	7	HAVCR1
Enterotoxin (CPE)	Aerolysin	β	*C. perfringens*	6	Claudin
Haemolytic lectin (LSL)	Aerolysin	β	*L. sulphureus*	4–6	Carbohydrates
Kysenin	Aerolysin	β	*E. fetida*	3–6	Sphingomyelin
Perfringolysin O (PFO)	CDCs	β	*C. perfringens*	30–50	Cholesterol
Suilysin (SLY)	CDCs	β	*S. suis*	30–50	Cholesterol
Intermedilysin (ILY)	CDCs	β	*S. intermedius*	30–50	Cholesterol, CD59
Listeriolysin O (LLO)	CDCs	β	*L. monocytogenes*	30–50	Cholesterol
Lectinolysin (LLY)	CDCs	β	*S. mitis*	30–50	Cholesterol, CD59
Anthrolysin O (ALO)	CDCs	β	*B. anthracis*	30–50	Cholesterol
Streptolysin O (SLO)	CDCs	β	*S. pyogenes*	30–50	Cholesterol
Plu-MACPF	MACPF	β	*P. luminescens*	>30	-
Bth-MACPF (BT 3439)	MACPF	β	*B. thetaiotaomicron*	>30	-
HlyA	RTX	α?	*E. coli*	-	-
Bifunctional haemolysin–adenylyl cyclase toxin (CyaA)	RTX	α?	*B. pertussis*	-	-
MARTX	RTX	α?	*A. hydrophila*	-	-

ADAM10, disintegrin and metalloproteinase domain-containing protein 10; *A. equina*, *Actinia equina*; *A. fragacea*, *Actinia fragacea*; *A. hydrophila*, *Aeromonas hydrophila*; *B. anthracis*, *Bacillus anthracis*; *B. cereus*, *Bacillus cereus*; *B. pertussis*, *Bordetella pertussis*; *B. thetaiotaomicron*, *Bacteroides thetaiotaomicron*; C5aR, C5a receptor; CCR5, CC-chemokine receptor type 5; CDC, cholesterol-dependent cytolysin; *C. perfringens*, *Clostridium perfringens*; CXCR1, CXC-chemokine receptor type 1; *E. coli*, *Escherichia coli*; *E. fetida*, *Eisenia fetida*; GPI, glycosylphosphatidylinositol; HAVCR1, hepatitis A virus cellular receptor 1; IM, bacterial inner membrane; *L. monocytogenes*, *Listeria monocytogenes*; LPS, lipopolysaccharide; *L. sulphurous*, *Laetiporus sulphurous*; MACPF, membrane attack complex component/perforin; MARTX, multifunctional autoprocessing repeats-in-toxin; OM, bacterial outer membrane; PC, phosphatidylcholine; PFT, pore-forming toxin; *P. luminescensis*, *Photorhabdus luminescens*; RTX, repeats-in-toxin; *S. aureus*, *Staphylococcus aureus*; *S. enterica*, *Salmonella enterica*; *S. flexneri*, *Shigella flexneri*; *S. helianthus*, *Stichodactyla helianthus*; *S. intermedius*, *Streptococcus intermedius*; *S. mitis*, *Streptococcus mitis*; *S. pyogenes*, *Streptococcus pyogenes*; *S. suis*, *Streptococcus suis*; *V. cholerae*, *Vibrio cholerae*; *V. vulnificus*, *Vibrio vulnificus*. *PFTs for which some structural data are available for the monomer and/or pore state; the list of receptors for each toxin is not exhaustive.

Box 2 | **Integrative modelling of pore structures**

X-ray crystallography has historically been the main source of high-resolution atomic structures of pore-forming toxins (PFTs). However, owing to the large size of the molecular assembly of each pore and the complexity of the pore formation process, alternative structural biology strategies are required to reveal the pore architecture and kinetics of oligomerization. To date, both the monomer and protomer conformation are known for only a handful of PFTs, but recent advances in cryo-electron microscopy (cryo-EM) promise to reveal the conformation of large toxin assemblies at higher resolution, as was recently exemplified by atomic-level resolution structures of the Tc toxin from *Photorhabdus luminescens*[115,116] and the anthrax toxin protective antigen[112]. In parallel, progress in the sophistication of molecular modelling has enabled the integration of experimental inputs from different sources (with different resolution and completeness) in consistent models of macromolecular complexes. In this context, optimization and simulation schemes have been developed to integrate high-resolution structures of individual components, their native dynamics[191–193] and low-resolution spatial data by a growing array of techniques (see the figure). This emerging approach is commonly known as integrative modelling[192,194,195] and has already helped to reveal the functional architecture of several macromolecular complexes[196,197], including the PFTs, suilysin[109] and pleurotolysin (a fungal toxin)[90], as well as aerolysin[75] and monalysin[198], which are both members of the aerolysin family and share the same pore architecture.

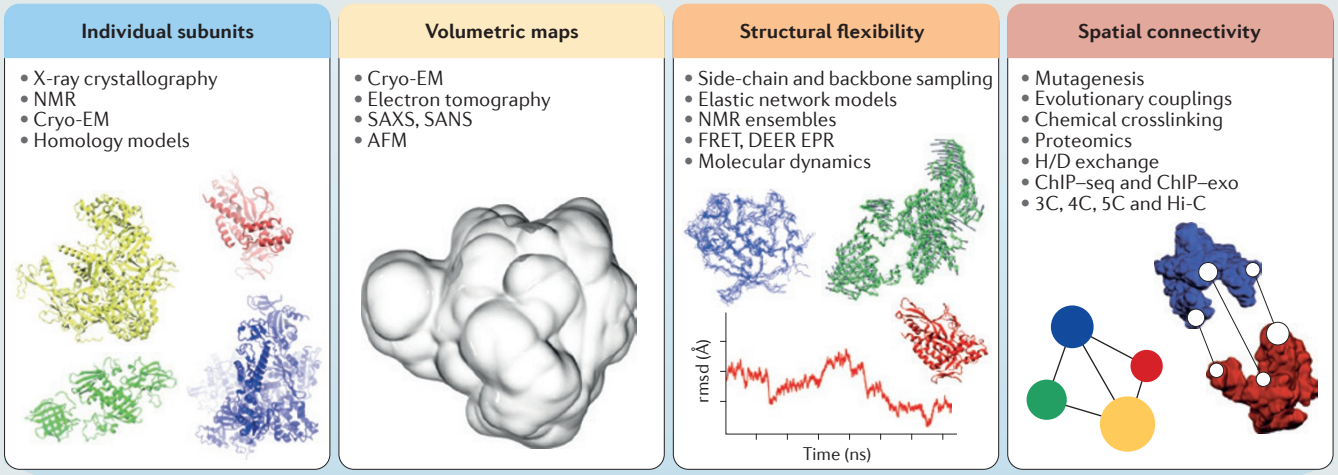

3C, chromatin conformation capture; 4C, circularized 3C; 5C, carbon-copy 3C; AFM, atomic force microscopy; ChIP–exo, ChIP–seq with an exonuclease sample preparation step; ChIP–seq, chromatin immunoprecipitation followed by sequencing; DEER EPR, double electron–electron resonance electron paramagnetic resonance; FRET, fluorescence resonance energy transfer; H/D exchange, hydrogen–deuterium exchange; NMR, nuclear magnetic resonance; Hi-C, genome-wide 3C; rmsd, root-mean-square deviation; SANS, small-angle neutron scattering; SAXS, small-angle X-ray scattering.

outer membrane vesicles (OMVs) of *E. coli*[39]. Pre-pore-containing OMVs would be protected from pore formation as the conformational changes leading to membrane insertion require cholesterol, which is generally not present in bacterial membranes. A similar OMV-mediated delivery mechanism of PFTs has recently been proposed for *Vibrio cholerae* cytolysin (VCC)[40], which belongs to the *Staphylococcus aureus* haemolysin family (see below). However, if pre-pores are indeed encapsulated within OMVs, it is not known how these OMV-embedded pre-pores would be delivered to the target membrane.

The actinoporin family. Actinoporins are eukaryotic proteins that are produced by sea anemones[41]. They form part of the venom that these sedentary animals rely on to paralyse and digest their prey (which range from plankton to fish and crustaceans), as well as to defend themselves from predators. By forming pores in the plasma membrane of target cells, actinoporins are thought to cause cell lysis.

X-ray structures have been reported for the soluble form of the actinoporins equinatoxin II (EqtII; produced by *Actinia equina*)[42,43], sticholysin II (StnII; produced by *Stichodactyla helianthus*)[44] and fragaceatoxin C (FraC; produced by *Actinia fragacea*)[45] (TABLE 1). All actinoporins are composed of a β-sandwich flanked by two α-helices (FIG. 2a), in which the N-terminal amphipathic helix detaches from the core of the protein and inserts into the membrane[41]. This membrane insertion step is lipid-dependent, with a preference for target membranes that are enriched in sphingomyelin and/or have phase-separated lipid membranes[41,46]. Interestingly, membrane insertion of

Outer membrane vesicles (OMVs). Vesicles that are derived from the outer membrane of Gram-negative bacteria.

Sphingomyelin
A sphingolipid found in animal cells that generally has a phosphocholine headgroup.

Phase-separated lipid membranes
Membranes within which lipids are separated into different domains.

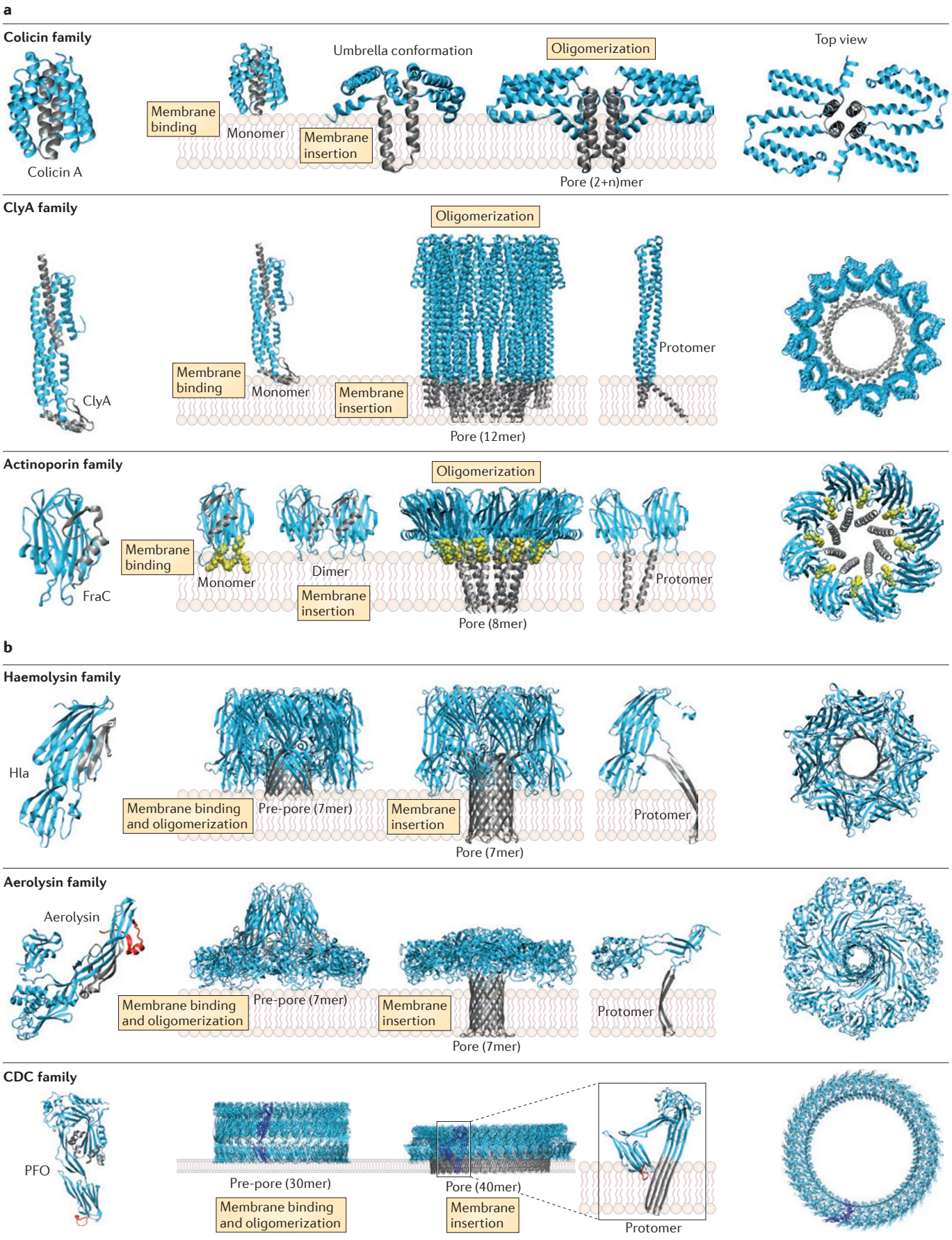

◀ Figure 2 | **Structural architectures and pore formation mechanisms of pore-forming toxin families.** Pore formation mechanisms for representative members of all six pore-forming toxin (PFT) families are illustrated using solved structures. For each pore, a model of an isolated protomer (or protomers) is also shown to highlight the membrane insertion event that underpins the transition of the PFT from a soluble state to a transmembrane conformation, which is a fundamental step in pore formation. Structural motifs that undergo membrane insertion are highlighted in grey. **a** | For α-PFTs (the colicin family, the cytolysin A (ClyA) family and the actinoporin family), monomers bind to the membrane in a step that precedes pore formation. Once bound to the membrane, pore formation relies on the extraction of α-helical domains from the monomer and subsequent insertion of the extracted domain into the membrane. The structure of the soluble form of colicin A has been solved (RCSB Protein Data Bank (PDB) entry 1COL)[14] and is shown here. For PFTs from this family, the extraction of the hydrophobic hairpin and its insertion into the membrane results in an 'umbrella' conformation that is thought to drive pore formation by inducing oligomerization into dimers[25] or higher-order assemblies of varied stoichiometries. The conformations of membrane-inserted colicin A shown in this figure are hypothetical models. The structure of ClyA has been solved in its soluble monomeric form (PDB entry 1QOY)[35] and mature dodecameric pore conformation (PDB entry 2WCD)[36], which are both shown in the figure. Structures of the actinoporin family PFT fragaceatoxin C (FraC) have been reported for the lipid-bound monomeric form (PDB entry 4TSL; lipids are shown in yellow), a dimeric intermediate (PDB entry 4TSN) and the mature octameric pore conformation (PDB entry 4TSY), which is intercalated with sphingomyelin moieties (shown in yellow)[50]. **b** | For β-PFTs (the haemolysin family, the aerolysin family and the cholesterol-dependent cytolysin (CDC) family), pore formation relies on the extraction of a pre-stem loop that inserts into the membrane where it ultimately combines with the extracted pre-stem loops of other protomers to form a β-barrel. The structure of α-haemolysin (Hla) from *Staphylococcus aureus* has been solved in monomeric conformation (PDB entry 4IDJ)[153] and single-component heptameric conformation (PDB entry 7AHL)[58]. After binding to the membrane, the pre-stem loop starts extracting to form a partial β-barrel, leading to a pre-pore state, the structure of which has been solved for γ-haemolysin (Hlg) and is shown in this figure (PDB entry 4P1Y)[59]. The pre-pore evolves into a mature pore by insertion of the complete β-barrel into the membrane. The haemolysin family also includes bi-component leukocidins, which form octameric pores that otherwise have a similar architecture. The structure of aerolysin has been solved in its soluble, monomeric form (PDB entry 1PRE[69]; the carboxy-terminal peptide that has to be cleaved for toxin activation is shown in red). Aerolysin first assembles in a pre-pore state and, after extraction of the pre-stem loop (in grey), it eventually reaches the heptameric pore conformation[75], as determined by integrative modelling (BOX 2). The structure of the CDC family PFT perfringolysin (PFO) has been solved in its monomeric form (PDB entry 1PFO[95]; the undecapeptide that binds to cholesterol is shown in red). PFOs oligomerize to form large pre-pores, which, after an extended conformational change, form a membrane-inserted β-barrel. The models of the high-order assemblies of CDCs that form the pre-pore and pore are as suggested in REF. 111; the stoichiometries of these structures can be highly variable according to the conditions.

Differential scanning calorimetry
A technique used to characterize the energetics associated with conformational changes of biomolecules, such as protein folding or phase transitions in lipid and lipid–protein mixtures upon temperature variation.

Atomic force microscopy
(AFM). A technique that uses the deflection of a sharp-tipped probe to measure the local conformation and mechanical properties of a sample (for example, proteins embedded in a membrane) with up to nanometre resolution.

actinoporins can subsequently induce lipid mixing, as has recently been shown for sticholysin using differential scanning calorimetry and atomic force microscopy (AFM)[47].

Membrane insertion of the N-terminal helix is followed by oligomerization and pore formation, with no pre-pore intermediate state[48]. The stoichiometry of the pores formed by these toxins varies from tetramers, which have been proposed for EqtII[49] and StnII[44], to nonamers, which have been proposed for FraC[45]. Until recently, the arrangement of proteins and lipids in the formation of actinoporin pores was unclear[41], but X-ray structures for FraC in its monomeric, dimeric and octameric states have illuminated not only the final pore conformation but also some novel details of the pore formation mechanism[50]. The FraC octameric pore is assembled in a 1:1 ratio with sphingomyelin, which not only acts as a receptor that recruits FraC to the membrane but is also an indispensable cofactor that is required to trigger and complete the assembly of the mature pore (FIG. 2a). Furthermore, the X-ray structure of a stable FraC dimer revealed conformational changes in the membrane-inserted N-terminal amphipathic helix towards the protomer state found in pores, which in turn suggested that actinoporin protomers might assemble sequentially into a pore in a mechanism that excludes the formation of the pre-pore intermediate states observed for many β-PFTs (see below).

β-PFTs

The haemolysin family. The opportunistic human pathogen *S. aureus*, a leading cause of pneumonia and sepsis[51], produces an arsenal of virulence factors. These virulence factors are encoded on mobile genetic elements, which leads to diverse toxin expression combinations in different infectious strains. The arsenal of *S. aureus* virulence factors includes several PFTs, which are either composed of a single component, as in the case of α-haemolysin (Hla), or of two components, as in the case of γ-haemolysin AB (HlgAB), HlgCB, leukocidin ED (LukED), Panton–Valentine leukocidin (PVL) and leukocidin AB (LukAB; also known as LukGH)[52] (TABLE 1). These PFTs are not functionally redundant and target different cell types, mostly in the immune system, by interacting with different cell surface proteins[10,52]. PFTs in the haemolysin family contribute to *S. aureus* pathogenesis in several ways: some will kill various cells of the immune system, as an immune evasion strategy, whereas others, such as Hla, also disrupt epithelial barriers, thus promoting bacterial dissemination.

All staphylococcal PFT components have a similar fold, which is also shared by the necrotic enteritis toxin B (NetB)[53], the δ-toxins[54] from *Clostridium perfringens* and VCC[55]. The single-component toxins of this family assemble into heptameric pores, whereas the bi-component toxins form octameric pores[56], containing four alternating copies of each subunit[57]. The haemolysin family is one of the best characterized PFT families in terms of structure, as Hla[58], Hlg[57,59], HlgB[60], VCC[55,61] and NetB[53] have all been crystallized in the soluble and/or the pore configuration (FIG. 2b). This abundance of structural data has enabled the production of consistent and reliable pore models based on homology, as is the case for the δ-toxin from *C. perfringens*[62]. In the soluble state, *S. aureus* haemolysins form a rather compact structure, rich in β-strands[58], in which the pre-stem domain (which subsequently becomes the transmembrane domain; FIG. 2b) forms a three-stranded β-sheet that is packed against the core of the protein. Following oligomerization into a heptameric or octameric pre-pore ring-like structure, the pre-stem domain (which localizes to the internal cavity of the ring) detaches from the core of the protein, readjusts into an anti-parallel β-hairpin and, in combination with neighbouring hairpins, generates a 14-stranded or 16-stranded β-barrel (FIG. 2b). As the outside of this barrel is hydrophobic, it spontaneously inserts into the lipid bilayer. Membrane insertion and formation of the amphipathic β-barrel are likely to be concomitant events. Note that, although it is essential for pore formation, the pre-stem loop is not required for oligomerization[63].

The aerolysin family. The aerolysin family is a broad family of PFPs. The first described member, aerolysin, is produced by Gram-negative *Aeromonas* spp.[64], and other bacterial aerolysins include the α-toxin produced by the Gram-positive human pathogen *Clostridium septicum*[65], monalysin produced by *Pseudomonas entomophila*[66] and several parasporins produced by *B. thuringiensis*[28]. In pathogens such as *Aeromonas hydrophila*, aerolysins contribute to bacterial dissemination, possibly through disruption of epithelial barriers, which would in some cases lead to deep wound infection[64].

Bioinformatics analysis has revealed that the core aerolysin motif, which is composed of pairs of two β-strands separated by the pre-stem domain, can be found in all kingdoms of life[7]. Eukaryotic aerolysins include: enterolobin from the seeds of the tree *Enterolobium contortisiliquum*[5], which is typically found in Brazil; biomphalysin produced by the snail *Biomphalaria glabrata*[8]; and βγ-CAT produced by the frog *Bombina maxima*[9]. Several aerolysin family members produced by animals have been shown to have a role in the immune system[8,9,67,68].

In contrast to *S. aureus* haemolysins, the soluble form of aerolysin is a highly elongated, multidomain protein[69] (FIG. 2b). At the high protein concentrations used for crystallography, aerolysin is dimeric[70]; in this form, the pre-stem region forms a β-strand-containing loop in the middle region of the elongated domain[71], as initially shown for *C. septicum* α-toxin[72]. An unusual feature of aerolysin is that it is synthesized as a protoxin[73] with a carboxy-terminal extension that prevents premature oligomerization[64,70]. Following cleavage of the C-terminal peptide, the toxin oligomerizes into heptameric ring-like structures[70,74].

Only recently, using a combination of X-ray crystallography, cryo-electron microscopy (cryo-EM), molecular dynamics and modelling (BOX 2), a near-atomic-level understanding of the pore-formation process was obtained for the aerolysin family[75] (FIG. 2b). Using aerolysin mutants arrested at different stages along the pathway leading to pore formation, the structure of the intermediate pre-pore state and the structure of the mature pore were solved[75]. Monomers first assemble into a heptameric pre-pore structure. This complex docks onto the membrane surface, with the pre-stem loops ready to slide through a pocket into the interior cavity of the pre-pore (FIG. 2b). Triggering the transition from pre-pore to pore, the pre-stem loops eventually refold into amphipathic β-hairpins forming the transmembrane β-barrel. This conformational change is accompanied by a concerted swirling mechanism that flattens the extracellular portion of the pore as the β-barrel forms and inserts into the membrane. Aerolysin pores thus have a large, flat, disc-like extracellular structure, which is somewhat elevated with respect to the membrane (FIG. 2b). Despite a different pore-formation process, a similar architecture of the final pore was recently found for the haemolytic lectin CEL-III produced by the sea cucumber *Cucumaria echinata*[76].

As amphipathic β-barrels could potentially move within or extrude from the membrane, different mechanisms have evolved to stabilize the barrel positioning. In the case of Hla produced by *S. aureus*, the cytosolic tip of the transmembrane β-hairpin has charged residues that anchor the tip in the cytosol, whereas the tips of the aerolysin transmembrane β-hairpins are hydrophobic and adopt a rivet-like configuration that prevents motion and anchors the barrel within the bilayer core[71]. Furthermore, the lumen of aerolysin β-barrels is markedly different from the lumen of *S. aureus* Hla, with a very high concentration of charged residues[75], which might favour the conduction of anionic moieties and increase pore flexibility.

The primary structure of proteins from the aerolysin family may show very little, if any, similarity to one another. Crystallographic studies, however, have revealed remarkable structural similarities in the fold of aerolysins with diverse primary sequences, such as *C. perfringens* ε-toxin[77,78], *C. perfringens* enterotoxin (CPE)[79–81], a haemolytic lectin (LSL) produced by the parasitic mushroom *Laetiporus sulphureus*[82], the hydralysin toxins produced by Cnidaria[83] and the lysenin toxin produced by the earthworm *Eisenia fetida*[84] (TABLE 1). Further studies on these proteins will establish whether they have the same global architecture as aerolysin and whether they share its swirling mechanism for membrane insertion.

The cholesterol-dependent cytolysin family. The cholesterol-dependent cytolysin (CDC) family is a large family of toxins mostly produced by Gram-positive bacteria of the *Bacillus*, *Clostridium*, *Streptococcus* and *Listeria* genera[85], and more recently shown to be produced by some Gram-negative bacteria[86]. Depending on the pathogen, these PFTs contribute to infection in different ways: listeriolysin O (LLO) mediates the release of *Listeria* spp. once the bacterium has entered the target cell through a phagocytic-like mechanism; perfringolysin O (PFO) has an important role in the development of gangrene, which is often associated with *C. perfringens* infections; and pneumolysin (Ply) is required for tissue invasion by *Streptococcus pneumoniae*, and also contributes to inflammation and activation of the complement cascade[85].

Structural studies have revealed that CDCs share the same fold as membrane attack complex component/perforin (MACPF) domains, which have primarily been described in the mammalian immune system[87–89]. MACPF domain proteins in non-mammalian eukaryotes include pleurotolysin in fungi[90], and perforin-like proteins in apicomplexan parasites such as *Toxoplasma gondii* and *Plasmodium falciparum*[91,92], which are involved in parasite release from the parasitophorous vacuole following replication. Although mainly described in eukaryotes, the MACPF fold has also been found in bacteria (for example, in Plu-MACPF from *Photorhabdus luminescens*[88], BT3439 from *Bacteroides thetaiotaomicron*[93] and BSAP-1 from *Bacteroides fragilis*[94]; TABLE 1). The precise role of these bacterial MACPF proteins in infection remains to be fully elucidated.

Lectin
One of a family of proteins that bind to sugar moieties in glycoproteins.

Parasitophorous vacuole
The endosome-like organelle in which parasites reside upon engulfment by the target cell.

Several CDCs have been crystallized in their soluble form: PFO[95], suilysin (SLY) produced by *Streptococcus suis*[96], intermedilysin (ILY) produced by *Streptococcus intermedius*[97], LLO produced by *Listeria monocytogenes*[98], lectinolysin (LLY) produced by *Streptococcus mitis*[99], anthrolysin O (ALO) produced by *Bacillus anthracis*[100] and streptolysin O (SLO) produced by *Streptococcus pyogenes*[101] (TABLE 1). However, no CDC has been crystallized in the pore configuration, owing to the stoichiometry of the complexes, in which up to 50 monomers assemble into very large ring-like structures. However, these structures are amenable to analysis by electron microscopy (EM)[102] and AFM[103], providing information on the pore architecture.

PFO, the archetypical toxin of this family, is an elongated, β-sheet-rich, multidomain protein[95] (FIG. 2b). As opposed to the single β-hairpin contributed by haemolysin- and aerolysin-like toxins, each CDC molecule contributes two amphipathic β-hairpins to the final β-barrel[104,105]. Remarkably, in the soluble form, these regions are organized as two pairs of short α-helices that flank a central β-sandwich. Upon oligomerization and membrane insertion, they undergo a prion-like α-helix-to-β-strand transition[104,105], a conversion that is also observed for the sea cucumber haemolytic lectin CEL-III[76]. The two β-hairpins subsequently arrange into a slightly curved β-sheet that joins with the neighbouring β-sheets in the oligomer to form a giant β-barrel composed of 80–200 β-strands, depending on the pore stoichiometry. Oligomerization of CDCs seems to occur by the sequential addition of monomers or multimers[106,107] (FIG. 2b); however, in some instances oligomerization fails to occur completely, leading to the formation of arc-like structures — partially formed, open pores of lower stoichiometry — that have been proposed to nevertheless be active pores[108] (FIG. 1). This was recently confirmed for SLY using a combination of cryo-EM, AFM and modelling techniques, which revealed a sequential mechanism of oligomerization that produces not only pores but also arc-like structures that are kinetically trapped at the pre-pore state. Both closed rings and incomplete arcs seem to share the ability to form active pores by excluding lipids[109].

Correct alignment of the β-strands is essential for pore assembly, especially for such a large complex. Using disulfide scanning, it was found that partially unfolded β-hairpins are highly dynamic in the pre-pore complex, whereas in the pore state the β-barrel conformation is locked, producing a ~20° tilt in the orientation of the β-strands with respect to the membrane[106]. A recent study revealed that the energy required for the pre-pore-to-pore transition is provided by the formation of a salt bridge between adjacent monomers at the completion of oligomerization[110]. This leads to the coordinated disruption of a critical interface within each monomer. In the transition from pre-pore to pore, CDCs undergo an elongation at the membrane surface, as was first observed using AFM[103]. Combining all available data, including EM analysis of CDCs, a molecular modelling study[111] led to the elucidation of a general mechanism for CDC pore formation, in which the observed collapse from the pre-pore to the pore state could be explained by the simple rotation of the core domain of the toxin (FIG. 2b), through a mechanism reminiscent of the swirling mechanism reported for aerolysin collapse[75]. A very similar pore architecture was found for mammalian perforins[89].

PFTs are generally defined as toxins for which pore formation represents the primary toxic activity. However, many other toxins have a pore-forming domain or subunit, which is used as a translocon to deliver a catalytic subunit with toxic activity into a target cell. As opposed to the effectors of bacterial secretion systems, bacterial toxins with pore-forming domains are autonomous, as a secretion system apparatus is not required for target cell entry. Although we do not review translocation domains of toxins in this article, it is worth mentioning two recent examples of studies that have revealed translocation pore architectures at atomic resolution. First, the transmembrane conformation of the translocation subunit (also known as the protective antigen (PA)) of the anthrax toxin was shown to form heptameric or octameric pores[112,113]. The most unusual feature of the anthrax pore is the extremely long 105 Å β-barrel. The lumen of the pore, which translocates the catalytic subunit, contains a structure known as a Φ-clamp[114] that ratchets the unfolded protein through the lumen[112] while ensuring that the pore remains impermeable to most ions. Second, in *P. luminescens*, binding of the TcB and TcC subunits of the Tc toxin complex to the TcA subunit was shown to induce the opening of the translocation channel of the toxin. The channel itself has a hydrophobic and narrow gate region similar to the anthrax Φ-clamp, which probably requires protein unfolding before translocation[115,116].

Specificity of PFTs

Each of the PFT families described in this Review is defined by a given fold and, presumably, a cognate membrane insertion mechanism. PFTs within a family, however, can have diverse target membranes, as they are produced by different organisms that target different cells for different purposes (BOX 1). Diversification has thus occurred in the domains specifically recognizing the host target membrane and associated receptors, as well as, to a lesser extent, in the residues that line the transmembrane pore (FIG. 3).

The sweet tooth of PFPs and PFTs. Many PFPs — and, in particular, many bacterial PFTs — bind to sugar molecules (FIG. 3a). For PFTs that target eukaryotic plasma membranes, these are usually glycans that are covalently attached to membrane-associated proteins or sugars that are present in the glycosylphosphatidylinositol (GPI) moiety in proteins with a GPI anchor. For example, in addition to the cytolytic domain it shares with *S. aureus* haemolysin, VCC has C-terminal domains with β-trefoil and β-prism folds[55]. The β-prism domain has lectin-like activity, as it interacts with β1-galactosyl-terminated glycoconjugates with nanomolar affinity[117]. This domain has been shown to be crucial for targeting erythrocyte membranes, by facilitating oligomerization and pore formation[117,118], although a specific receptor for VCC has not yet been identified. Similarly, *Vibrio vulnificus*

Disulfide scanning
An approach in which each amino acid in a sequence of interest is sequentially mutated to cysteine using a single point mutation. The reactivity of the introduced cysteine is analysed, for example, using a functional assay, to assess the dynamic location of the amino acid in the protein structure.

Translocon
A protein channel that enables the translocation of client proteins across a membrane.

GPI anchor
A glycosylphosphatidylinositol (GPI) lipid that is covalently linked to the carboxy terminus of a peripheral protein. The anchor attaches the protein to the outer leaflet of the plasma membrane.

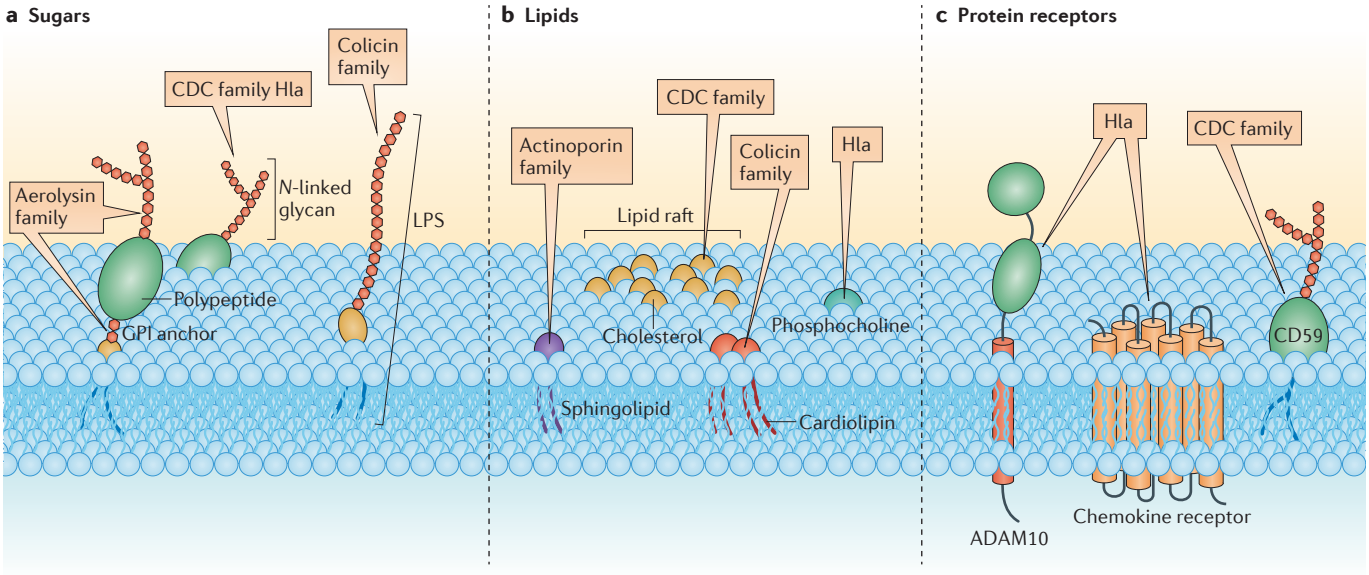

Figure 3 | **Specificity of pore-forming toxins.** Pore-forming toxins (PFTs) from different families recognize their target host cells with high specificity, largely owing to interactions with sugars, lipids and protein receptors at the target membrane. **a** | β-PFTs strongly interact with sugar moieties that protrude from the target membrane, where they are covalently attached to membrane proteins or, in Gram-negative bacterial outer membranes, lipids. For example, α-haemolysin (Hla) and PFTs from the cholesterol-dependent cytolysin (CDC) family bind to *N*-linked glycan modifications of proteins, and aerolysin binds to two sugar moieties on proteins with glycosylphosphatidylinositol (GPI) anchors, the glycan core of the anchor and *N*-linked glycans. Recently, colicins from the α-PFT family, which are both produced by and target *Escherichia coli*, have been reported to target lipopolysaccharides (LPS) in the outer bacterial membrane. **b** | Both α-PFTs and β-PFTs recognize specific lipid constituents of the target membrane. Fragaceatoxin C (FraC), which is an α-PFT from the actinoporin family, specifically recognizes sphingomyelin, whereas colicins seem to sense the anionic phospholipids, such as cardiolipins, that are abundant in the inner bacterial membrane. Hla, which is a β-PFT, has a specific binding site for phosphocholines, whereas β-PFTs in the CDC family have a high affinity for cholesterol and tend to oligomerize in lipid raft domains. **c** | β-PFTs, in particular, have been reported to bind to various protein receptors embedded in the membrane of host cells (often cells of the immune system), although the identity of most of these protein receptors remains unknown. Hla and CDCs are two exceptions for which a receptor is known; Hla interacts with the first extracellular domain of disintegrin and metalloproteinase domain-containing protein 10 (ADAM10) and with chemokine receptors, and CDCs have high affinity for CD59. Although CD59 is a GPI-anchored protein, as shown, CDC binding does not depend on the GPI anchor.

haemolysin (VVH) has multiple binding preferences, including glycerol, *N*-acetyl-D-galactosamine and *N*-acetyl-D-lactosamine, which enables it to recognize various cell surfaces[119].

Aerolysin binds to the target membrane through its first N-terminal domain, which protrudes from the elongated core of the protein (FIG. 2b). In an interesting dual-sugar binding mechanism, these domains bind to *N*-linked sugars[64,120] and to the glycan anchor of GPI-anchored proteins[70,121], collectively leading to a very-high-affinity interaction (FIG. 3a). In other toxins in this family, such as *C. perfringens* ε-toxin[122], *C. perfringens* enterotoxin[79], lysenin[84], haemolytic lectin[82] and parasporin[123], these two domains are replaced by domains with entirely different folds that are expected to correspond to different cognate target receptors. Although only a small number of receptors have been identified for aerolysin-like toxins, it has been shown that *C. perfringens* ε-toxin binds to an extensively *O*-linked glycoprotein, hepatitis A virus cellular receptor 1 (HAVCR1)[124]; it is thought that the binding site for ε-toxin on HAVCR1 is one of the sugar components of this glycoprotein. Another possible binding site on a sugar component of HAVCR1 was identified for the low-hazard H149A mutant variant of ε-toxin. This second binding site corresponded to the location of a β-octyl-glucoside glycan moiety in co-crystal structures of ε-toxin and HAVCR1 (REF. 125). CDCs were also recently found to bind to glycans, in addition to, or before, binding to cholesterol[126].

PFTs that target bacteria have been shown to have affinity for sugars that are covalently attached to lipids in bacterial membranes. For example, colicin N (ColN), which is secreted by — and active against — *E. coli*, binds to bacterial outer membrane lipopolysaccharides (LPS) (FIG. 3a; TABLE 1) as high-affinity receptors before translocating through outer membrane porin proteins to the inner membrane[127]. Some eukaryotic PFPs also bind to sugars in bacterial membranes, such as bactericidal C-type lectins present in the human gut, which bind to peptidoglycan carbohydrates to form hexameric pores in Gram-positive bacteria[128].

Affinity for lipids and lipid domains. Many PFTs have an affinity for specific lipids or lipid domains[129] (FIG. 3b). A role for lipid rafts in the pore-formation process was initially proposed for aerolysin[130], which has also been

Lipid rafts
Microscale or nanoscale domains of biological membranes that are rich in cholesterol and sphingolipids.

shown to bind to lipid-anchored proteins (although this interaction is mediated by *N*-linked glycan sugars)[64]. Another PFT from the aerolysin family, lysenin, which is produced by earthworms, specifically binds to sphingomyelin[131], which is enriched in lipid rafts. CDCs, as their name indicates, require cholesterol — another lipid enriched in lipid rafts — and therefore tend to oligomerize in lipid raft-like domains[132]. For instance, PFO oligomerization is dependent on the concentration of cholesterol in the target membrane. The composition and, in particular, the leaflet asymmetry of the target membrane seem to be crucial both to maintain the required cholesterol concentration and to stabilize the intermediate states of the membrane-inserted toxin during CDC pore formation[133]. These observations are intriguing, as they hint at the possibility that pore formation can be modulated by controlling the lipid composition of the two membrane leaflets. Cholesterol interaction is mediated by the undecapeptide ECTGLAWEWWR[134], which is one of the most conserved sequences among CDCs (FIG. 2b). As recently shown for PFO, this peptide also provides allosteric coupling, as cholesterol-mediated membrane binding promotes oligomerization[135]. The lytic activity of CDCs may be modulated by the interaction of the undecapeptide with neighbouring cholesterol-sensing domains, as recently found for SLO[101]. A second motif, composed of a threonine–leucine pair (T490–L491), also mediates the recognition of, and binding to, cholesterol by PFO; this motif is highly conserved in the CDC family[136]. The most striking example of lipid specificity is seen in the sea anemone toxin FraC. As mentioned previously, sphingomyelin is a constitutive cofactor for the assembly of the FraC pore (FIG. 2a); furthermore, four distinct lipid-binding sites in this toxin modulate membrane binding with different affinity and specificity[50].

Lipid specificity has also been reported for lipids not directly associated with rafts. In the haemolysin family, *S. aureus* Hla has phosphocholine binding pockets, which are also found, in a modified form, in the NetB toxin produced by *C. perfringens*[53]. Finally, lipid specificity has been reported in PFTs that target bacterial membranes. For colicins, the presence of anionic lipid species, such as cardiolipin, in the bacterial inner membrane seems to promote the formation of the umbrella conformation and conductive pores[23] (FIG. 3b; TABLE 1).

Affinity for protein receptors. In addition to sugars and lipids, some PFTs require interactions with host membrane proteins to target the host cell membrane (FIG. 3c); that is, these PFTs recognize the polypeptide chain itself, in addition to (or instead of) sugar moieties that are covalently attached to the protein. This additional specificity is particularly important for *S. aureus*, which specifically targets subsets of cells in the host immune system through the expression of PFTs that bind to receptors that are expressed only on specific cell types[10,52]. The bi-component LukED targets macrophages, dendritic cells and T cells by binding to CC-chemokine receptor type 5 (CCR5)[137] (TABLE 1) or neutrophils and monocytes by binding to CXC-chemokine receptor type 1 (CXCR1) and CXCR2 (REF. 138), whereas PVL binds to C5a receptors (C5aRs) to target neutrophils and, to a lesser extent, to target monocytes and macrophages[139]. The γ-bi-component haemolysins AB and CB (HlgAB, HlgCB) bind to the chemokine receptors CXCR1, CXCR2 and CCR2, and to the complement receptors C5aR and C5L2, respectively, to target neutrophils and monocytes[140]. Finally, Hla targets epithelial cells by binding to disintegrin and metalloproteinase domain-containing protein 10 (ADAM10)[141,142], in addition to phosphocholine head groups (TABLE 1).

Some CDCs, such as ILY, bind to the protein receptor CD59 (REFS 135,143), which is a potent inhibitor of the complement cascade, although cholesterol is still required for pore formation[144] (TABLE 1). ILY has recently been crystallized in its soluble monomeric form in complex with human CD59, revealing that the toxin binds to CD59 on two distinct interfaces, thus producing an optimal alignment to interact with the cholesterol-rich membrane and adjacent protomers for pre-pore formation[97]. These structural data enabled the design of ILY-derived peptides that were able to disrupt the interaction with CD59; structure-guided design of receptor-binding peptides thus holds promise for therapeutic development.

Therapeutic development

The growing characterization of the structure and function of PFTs and PFPs has enabled the development of biotechnological applications that target and engineer these proteins, including antimicrobial drug development, cancer gene therapy[145] and DNA sequencing[146,147].

The knowledge of conformational rearrangements and protomer interfaces established upon pore formation in PFTs can be applied to a traditional structure-based drug discovery approach, in which high-affinity small compounds are identified that target structural features to block pore formation and impair bacterial virulence (FIG. 4a). For example, it was shown that natural compounds, such as oroxylin A, oroxin A and oroxin B, inhibit the haemolytic activity of Hla, probably by blocking loop transition upon pore formation[148,149]. This inhibitory mechanism could aid in the design and development of anti-virulence agents to treat infections with multidrug-resistant strains of *S. aureus*. Similarly, DNA aptamers have been designed that specifically target the cytotoxic activity of Hla to inhibit *S. aureus* infections[150]. The identification of conformational rearrangements and protomer interfaces that are crucial for oligomerization and pore formation in other PFTs[151] may enable the structure-based design of drugs that prevent pore formation for a given toxin.

A structure-based strategy could also be used to prevent the binding of PFTs to their specific receptors (FIG. 4a). For PFTs in the aerolysin family, synthetic GPI molecules and GPI analogues have been proposed as inhibitors of pore assembly by preventing the correct attachment of the PFT to the plasma membrane[152]. Equally of note is the potential of therapeutic antibodies to impair pore formation by a similar mechanism. It has recently been shown that some individuals possess high-affinity neutralizing antibodies against *S. aureus* Hla that target the

DNA aptamers
Short oligonucleotides engineered and selected to specifically bind to target molecules with high affinity. As with antibodies (their protein counterparts), DNA aptamers have broad applications both in biotechnology and therapeutics.

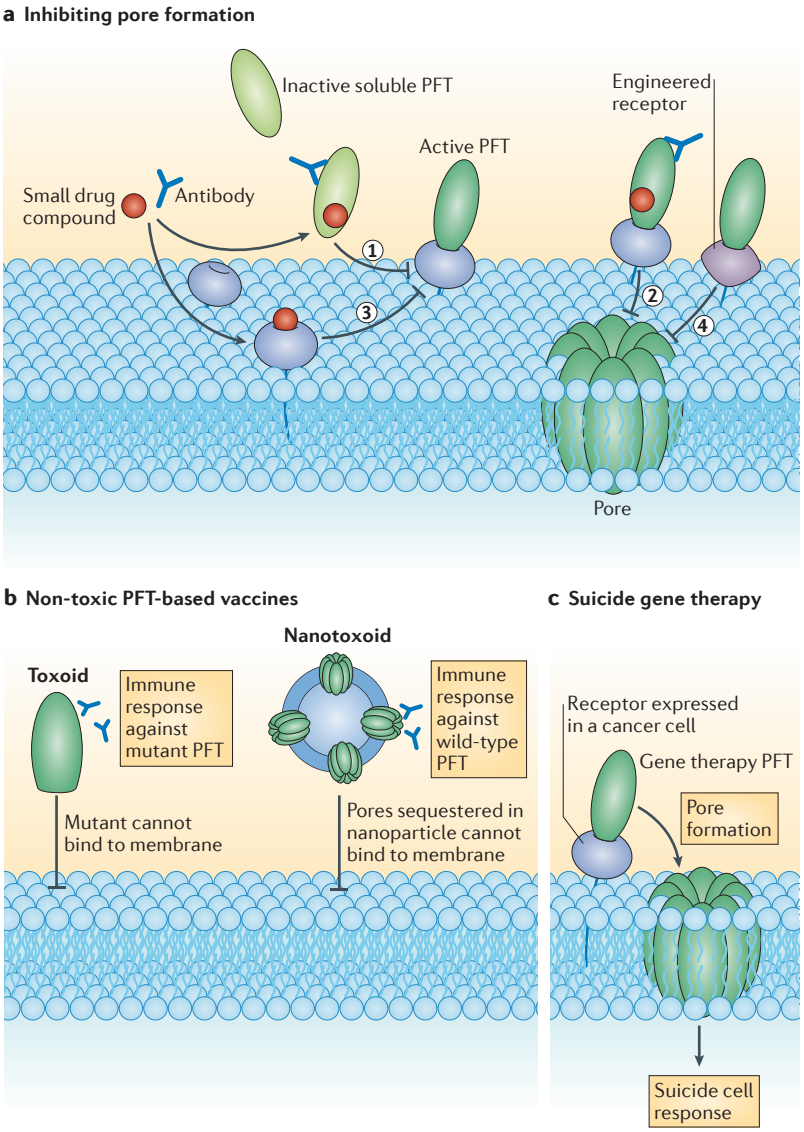

Figure 4 | **Therapeutic intervention.** A deeper understanding of the mechanisms of action of pore-forming toxins (PFTs) has led to new opportunities for the development of therapeutic remedies. **a** | Small drug molecules (such as oroxylin A, which inhibits α-haemolysin (Hla)) or engineered antibodies can be designed to target specific sites in PFTs that are involved in binding to the membrane (mechanism 1) and/or pore assembly (mechanism 2). Alternatively, small molecules can be identified that target the specific membrane receptors used by different PFTs (mechanism 3), impairing pore formation at the earliest steps by preventing the recruitment of the PFT to the membrane. An example of such a compound is maraviroc, which is an antagonist of the leukocidin ED (LukED) receptor CC-chemokine receptor type 5 (CCR5). Finally, specific receptors can be synthetically produced to sequester PFTs, thereby preventing complete oligomerization and pore insertion (mechanism 4). All of these strategies result in the inhibition of pore formation and, consequently, of the cellular response to membrane permeabilization. **b** | PFTs have also been used as a basis for vaccine development for microbial infections. Engineered PFTs with reduced virulence (known as toxoids) are able to promote an immune response. A recent innovation has enhanced this immune response even further by embedding fully active PFT pores (such as Hla pores) into nanoparticles coated with membrane bilayers, which render the pores non-toxic. The resulting 'nanotoxoid' complexes promote a stronger immune response than toxoids because they present wild-type proteins as antigens. **c** | Suicide gene therapy exploits the ability of PFTs to bind to specific receptors that are upregulated in cancer cells. The PFT is delivered by gene therapy and targets the cancer cells expressing these receptors, in which pore formation promotes a suicide response.

cap and rim domains; this is expected to impede receptor binding and membrane recognition[153]. Although the mechanism underlying the protective action of these antibodies requires further investigation, these results open the way to the development of interesting, novel therapeutics for bacterial infections that target PFTs.

As a reverse strategy, the receptor — rather than the cognate PFT — could be targeted, as in the case of ADAM10 for Hla[154] or CCR5 for LukED toxins. For CCR5, antagonists such as maraviroc were shown to block LukED-dependent cell death, and CCR5-deficient mice were resistant to infection with a strain of *S. aureus* that was lethal in wild-type mice, highlighting the therapeutic potential of targeting CCR5 (REF. 137). However, it should be noted that broadly targeting leukocidin receptors could have harmful repercussions on the activation of the immune system, and so the value of this approach as a therapeutic strategy is unclear.

Another antimicrobial strategy that targets PFTs is the use of PFTs with reduced toxicity as recombinant toxoid vaccines that trigger an immune response (FIG. 4b). Knowledge of toxin structure and pore architecture can be beneficial in this scenario, enabling the rational design of site-directed mutations that reduce host membrane binding and cytotoxic efficiency while introducing minimal antigenic modifications, as recently shown for variants of NetB[155] and ε-toxin[156]. Ply, a CDC that is produced by *S. pneumoniae*, has long been studied for toxoid vaccine development, recently resulting in promising pneumolysoid candidates, including the Ply mutant known as Δ6PLY[157] and proteins produced by genetic fusion with other pneumococcal proteins, such as pneumococcal surface adhesin A (PsaA)[158] and choline-binding protein A (CbpA)[159].

Possibly more promising is the use of nanoparticles coated with red blood cell membranes that act as sinks for PFTs, which enables the non-toxic use of wild-type PFTs and thus preserves antigen presentation (FIG. 4b). The resulting complex, known as a nanotoxoid, can thus be used *in vivo* to trigger an effective immune response, as recently shown for nanoparticles with *S. aureus* Hla pores[160,161]. Given the ubiquitous presence of PFTs in the most pathogenic bacteria, the development of nanotoxoid vaccines may have the potential to soon address the urgent need for new treatments that are effective against antibiotic-resistant infections.

From a different clinical perspective, the induction of cell death following pore formation can be exploited to promote suicide in malignant cancer cells (FIG. 4c); this has been shown by transfecting the gene encoding SLO into several cancer cell lines[145], which demonstrated the potential of this PFT for application in suicide gene therapy. Similarly, suicide gene therapy has successfully been used to target tumours overexpressing claudin 3, claudin 4 (REF. 162) and claudin 6 (REF. 163), which are receptors for CPE[164].

Summary and conclusions

PFTs are sophisticated and widely spread virulence factors produced by pathogenic bacteria. They disrupt epithelial barriers and modulate or kill cells of the

Toxoids
Bacterial toxins engineered to decrease virulence. Toxoids are used as vaccines for microbial infections as they contribute to the development of an immune response against the native toxin.

host immune system, thereby contributing to bacterial dissemination and growth, and trigger complex cellular responses that remain incompletely characterized (BOX 1). All PFTs undergo a functional metamorphosis that leads inactive, soluble and monomeric proteins to assemble into conductive transmembrane pores at the target cell membrane (FIG. 1). However, as advances in the past decade have shown, each of the six PFT families has a distinct structural fold, pore architecture and mechanism of membrane insertion (FIG. 2; TABLE 1). Furthermore, the identification of lipids, sugars and protein receptors that bind to PFTs has furthered our understanding of the determinants of host cell specificity (FIG. 3). Collectively, these molecular insights have enabled the design of therapeutics that interfere with pore formation and could thus be used to treat infections, potentially as a component of combination treatments.

Structural studies have revealed that, to combat microbial infections, the immune systems of various animals make use of PFPs that have similar structures to the PFTs used by microorganisms to attack hosts. The most recent example is the identification of aerolysin family members in the frog species *B. maxima*, which has an immune system very similar to that of mammals[67]. βγ-CAT, which contains an aerolysin-like protein domain[68], protects *B. maxima* against microbial infections[9] in the bacteria-rich mud pools in which the frog lives. Similarly, immune cells in the snail *B. glabrata* produce biomphalysin to kill *Schistosoma mansoni* sporocysts[8]. It is likely that the structural characterization of future PFPs that are identified in animals will highlight interesting variations in mechanisms used to achieve target specificity.

Some PFTs remain unclassified orphans, such as the PFT subfamily of the repeats-in-toxin (RTX) family of proteins, which have numerous glycine–aspartate-rich repeats involved in calcium binding[165]. PFTs in this RTX subfamily include HlyA, which is produced by various *E. coli* species; the bifunctional haemolysin–adenylyl cyclase (CyaA) toxin produced by *Bordetella pertussis*[165]; and the multifunctional autoprocessing repeats-in-toxin (MARTX) family of toxins produced by *A. hydrophila* and several other pathogens[166]. Very little is known about the structure and mechanism of RTX toxins, as they need to be purified using high concentrations of chaotropic agents and, as a result, they have been unamenable to crystallographic analysis. The only structural hint derives from the prediction of nine amphipathic α-helices, thought to be responsible for pore formation, in the N-terminal domain of HlyA[167].

The structural characterization of PFTs has recently revealed new conformations in the pore formation pathway. Therefore, for most PFT families, we now have a fairly clear view of the pore architecture at different stages of pore formation. The main challenges ahead are to comprehensively characterize the kinetics of this process and to design therapeutics — antibodies, drugs, peptides or nanotoxoids — that may inhibit its effects (FIG. 4). Finally, understanding how cells sense the changes in cytoplasmic ion composition that result from pore formation and how they respond to these changes at a molecular level will undoubtedly reveal novel mechanisms of membrane repair and danger sensing. As such, PFTs exemplify the value of studying bacterial virulence as a tool to elucidate the mechanisms underlying basic cellular functions.

1. Los, F. C., Randis, T. M., Aroian, R. V. & Ratner, A. J. Role of pore-forming toxins in bacterial infectious diseases. *Microbiol. Mol. Biol. Rev.* **77**, 173–207 (2013).
2. Bischofberger, M., Iacovache, I. & van der Goot, F. G. Pathogenic pore-forming proteins: function and host response. *Cell Host Microbe* **12**, 266–275 (2012).
3. Alves, G. G., Machado de Avila, R. A., Chavez-Olortegui, C. D. & Lobato, F. C. *Clostridium perfringens* ε-toxin: the third most potent bacterial toxin known. *Anaerobe* **30**, 102–107 (2014).
4. Lesieur, C., Vecsey-Semjn, B., Abrami, L., Fivaz, M. & van der Goot, F. G. Membrane insertion: the strategy of toxins. *Mol. Membrane Biol.* **14**, 45–64 (1997).
5. Iacovache, I., Bischofberger, M. & van der Goot, F. G. Structure and assembly of pore-forming proteins. *Curr. Opin. Struct. Biol.* **20**, 241–246 (2010).
6. Gouaux, E. Channel-forming toxins: tales of transformation. *Curr. Opin. Struct. Biol.* **7**, 566–573 (1997).
7. Szczesny, P. *et al.* Extending the aerolysin family: from bacteria to vertebrates. *PLoS ONE* **6**, e20349 (2011).
This study extended the boundaries of the aerolysin family beyond bacteria to a species range that encompasses all kingdoms of life.
8. Galinier, R. *et al.* Biomphalysin, a new β pore-forming toxin involved in *Biomphalaria glabrata* immune defense against *Schistosoma mansoni*. *PLoS Pathog.* **9**, e1003216 (2013).
9. Xiang, Y. *et al.* Host-derived, pore-forming toxin-like protein and trefoil factor complex protects the host against microbial infection. *Proc. Natl Acad. Sci. USA* **111**, 6702–6707 (2014).
10. Alonzo, F. & Torres, V. J. The bicomponent pore-forming leucocidins of *Staphylococcus aureus*. *Microbiol. Mol. Biol. Rev.* **78**, 199–230 (2014).
11. Diabate, M. *et al. Escherichia coli* α-hemolysin counteracts the anti-virulence innate immune response triggered by the rho GTPase activating toxin CNF1 during bacteremia. *PLoS Pathog.* **11**, e1004732 (2015).
12. Lakey, J. H., van der Goot, F. G. & Pattus, F. All in the family: the toxic activity of pore-forming toxins. *Toxicology* **87**, 85–108 (1994).
13. Cascales, E. *et al.* Colicin biology. *Microbiol. Mol. Biol. Rev.* **71**, 158–229 (2007).
14. Parker, M. W., Pattus, F., Tucker, A. D. & Tsernoglou, D. Structure of the membrane-pore-forming fragment of colicin A. *Nature* **337**, 93–96 (1989).
This article shows the first structure of the soluble form of a PFT, which provided new insights into the mechanism of pore formation.
15. Lakey, J. H. *et al.* Membrane insertion of the pore-forming domain of colicin A. A spectroscopic study. *Eur. J. Biochem.* **196**, 599–607 (1991).
16. Ridley, H., Johnson, C. L. & Lakey, J. H. Interfacial interactions of pore-forming colicins. *Adv. Exp. Med. Biol.* **677**, 81–90 (2010).
17. Parker, M. W., Tucker, A. D., Tsernoglou, D. & Pattus, F. Insights into membrane insertion based on studies of colicins. *Trends Biochem. Sci.* **15**, 126–129 (1990).
18. Parker, M. W., Postma, J. P., Pattus, F., Tucker, A. D. & Tsernoglou, D. Refined structure of the pore-forming domain of colicin A at 2.4 Å resolution. *J. Mol. Biol.* **224**, 639–657 (1992).
19. Kienker, P. K., Qiu, X., Slatin, S. L., Finkelstein, A. & Jakes, K. S. Transmembrane insertion of the colicin Ia hydrophobic hairpin. *J. Membr. Biol.* **157**, 27–37 (1997).
20. Kim, Y., Valentine, K., Opella, S. J., Schendel, S. L. & Cramer, W. A. Solid-state NMR studies of the membrane-bound closed state of the colicin E1 channel domain in lipid bilayers. *Protein Sci.* **7**, 342–348 (1998).
21. Tory, M. C. & Merrill, A. R. Adventures in membrane protein topology. A study of the membrane-bound state of colicin E1. *J. Biol. Chem.* **274**, 24539–24549 (1999).
22. Shin, Y. K., Levinthal, C., Levinthal, F. & Hubbell, W. L. Colicin E1 binding to membranes: time-resolved studies of spin-labeled mutants. *Science* **259**, 960–963 (1993).
23. Pulagam, L. P. & Steinhoff, H. J. Acidic pH-induced membrane insertion of colicin A into *E. coli* natural lipids probed by site-directed spin labeling. *J. Mol. Biol.* **425**, 1782–1794 (2013).
24. Slatin, S. L., Qiu, X. Q., Jakes, K. S. & Finkelstein, A. Identification of a translocated protein segment in a voltage-dependent channel. *Nature* **371**, 158–161 (1994).
25. Dunkel, S., Pulagam, L. P., Steinhoff, H. J. & Klare, J. P. *In vivo* EPR on spin labeled colicin A reveals an oligomeric assembly of the pore-forming domain in *E. coli* membranes. *Phys. Chem. Chem. Phys.* **17**, 4875–4878 (2015).
26. Greig, S. L., Radjainia, M. & Mitra, A. K. Oligomeric structure of colicin ia channel in lipid bilayer membranes. *J. Biol. Chem.* **284**, 16126–16134 (2009).
27. Choe, S. *et al.* The crystal structure of diphtheria toxin. *Nature* **357**, 216–222 (1992).
28. Xu, C., Wang, B. C., Yu, Z. & Sun, M. Structural insights into *Bacillus thuringiensis* Cry, Cyt and parasporin toxins. *Toxins (Basel)* **6**, 2732–2770 (2014).
29. Barta, M. L. *et al.* The structures of coiled-coil domains from type III secretion system translocators reveal homology to pore-forming toxins. *J. Mol. Biol.* **417**, 395–405 (2012).

30. Westphal, D., Dewson, G., Czabotar, P. E. & Kluck, R. M. Molecular biology of Bax and Bak activation and action. *Biochim. Biophys. Acta* **1813**, 521–531 (2011).
31. Garcia-Saez, A. J., Fuertes, G., Suckale, J. & Salgado, J. Permeabilization of the outer mitochondrial membrane by Bcl-2 proteins. *Adv. Exp. Med. Biol.* **677**, 91–105 (2010).
32. Hunt, S., Green, J. & Artymiuk, P. J. Hemolysin E (HlyE, ClyA, SheA) and related toxins. *Adv. Exp. Med. Biol.* **677**, 116–126 (2010).
33. Madegowda, M., Eswaramoorthy, S., Burley, S. K. & Swaminathan, S. X-ray crystal structure of the B component of hemolysin BL from *Bacillus cereus*. *Proteins* **71**, 534–540 (2008).
34. Jessberger, N., Dietrich, R., Bock, S., Didier, A. & Martlbauer, E. *Bacillus cereus* enterotoxins act as major virulence factors and exhibit distinct cytotoxicity to different human cell lines. *Toxicon* **77**, 49–57 (2014).
35. Wallace, A. J. *et al. E. coli* hemolysin E (HlyE, ClyA, SheA): X-ray crystal structure of the toxin and observation of membrane pores by electron microscopy. *Cell* **100**, 265–276 (2000).
36. Mueller, M., Grauschopf, U., Maier, T., Glockshuber, R. & Ban, N. The structure of a cytolytic α-helical toxin pore reveals its assembly mechanism. *Nature* **459**, 726–730 (2009).
This paper reports the first atomic-resolution structure of an α-PFT pore, revealing the complex protomer rearrangement required for pore assembly.
37. Ganash, M. *et al.* Structure of the NheA component of the Nhe toxin from *Bacillus cereus*: implications for function. *PLoS ONE* **8**, e74748 (2013).
38. Vaidyanathan, M. S., Sathyanarayana, P., Maiti, P. K., Visweswariah, S. S. & Ayappa, K. G. Lysis dynamics and membrane oligomerization pathways for Cytolysin A (ClyA) pore-forming toxin. *RSC Adv.* **4**, 4930–4942 (2014).
39. Fahie, M. *et al.* A non-classical assembly pathway of *Escherichia coli* pore-forming toxin cytolysin A. *J. Biol. Chem.* **288**, 31042–31051 (2013).
40. Elluri, S. *et al.* Outer membrane vesicles mediate transport of biologically active *Vibrio cholerae* cytolysin (VCC) from *V. cholerae* strains. *PLoS ONE* **9**, e106731 (2014).
41. Kristan, K. C., Viero, G., Dalla Serra, M., Macek, P. & Anderluh, G. Molecular mechanism of pore formation by actinoporins. *Toxicon* **54**, 1125–1134 (2009).
42. Hinds, M. G., Zhang, W., Anderluh, G., Hansen, P. E. & Norton, R. S. Solution structure of the eukaryotic pore-forming cytolysin equinatoxin II: implications for pore formation. *J. Mol. Biol.* **315**, 1219–1229 (2002).
43. Athanasiadis, A., Anderluh, G., Macek, P. & Turk, D. Crystal structure of the soluble form of equinatoxin II, a pore-forming toxin from the sea anemone *Actinia equina*. *Structure* **9**, 341–346 (2001).
44. Mancheno, J. M., Martin-Benito, J., Martinez-Ripoll, M., Gavilanes, J. G. & Hermoso, J. A. Crystal and electron microscopy structures of sticholysin II actinoporin reveal insights into the mechanism of membrane pore formation. *Structure* **11**, 1319–1328 (2003).
45. Mechaly, A. E. *et al.* Structural insights into the oligomerization and architecture of eukaryotic membrane pore-forming toxins. *Structure* **19**, 181–191 (2011).
46. Barlic, A. *et al.* Lipid phase coexistence favors membrane insertion of equinatoxin-II, a pore-forming toxin from *Actinia equina*. *J. Biol. Chem.* **279**, 34209–34216 (2004).
47. Ros, U. *et al.* The sticholysin family of pore-forming toxins induces the mixing of lipids in membrane domains. *Biochim. Biophys. Acta* **1828**, 2757–2762 (2013).
48. Rojko, N. *et al.* Membrane damage by an α-helical pore-forming protein, equinatoxin II, proceeds through a succession of ordered steps. *J. Biol. Chem.* **288**, 23704–23715 (2013).
49. Baker, M. A., Rojko, N., Cronin, B., Anderluh, G. & Wallace, M. I. Photobleaching reveals heterogeneous stoichiometry for equinatoxin II oligomers. *Chembiochem* **15**, 2139–2145 (2014).
50. Tanaka, K., Caaveiro, J. M., Morante, K., Gonzalez-Manas, J. M. & Tsumoto, K. Structural basis for self-assembly of a cytolytic pore lined by protein and lipid. *Nat. Commun.* **6**, 6337 (2015).
This study shows the importance of sphingomyelin lipids for the integral assembly of the final PFT pore structure.
51. Schreiber, M. P., Chan, C. M. & Shorr, A. F. Bacteremia in *Staphylococcus aureus* pneumonia: outcomes and epidemiology. *J. Crit. Care* **26**, 395–401 (2011).
52. DuMont, A. L. & Torres, V. J. Cell targeting by the *Staphylococcus aureus* pore-forming toxins: it's not just about lipids. *Trends Microbiol.* **22**, 21–27 (2014).
53. Savva, C. G. *et al.* Molecular architecture and functional analysis of NetB, a pore-forming toxin from *Clostridium perfringens*. *J. Biol. Chem.* **288**, 3512–3522 (2013).
54. Keyburn, A. L., Bannam, T. L., Moore, R. J. & Rood, J. I. NetB, a pore-forming toxin from necrotic enteritis strains of *Clostridium perfringens*. *Toxins* **2**, 1913–1927 (2010).
55. De, S. & Olson, R. Crystal structure of the *Vibrio cholerae* cytolysin heptamer reveals common features among disparate pore-forming toxins. *Proc. Natl Acad. Sci. USA* **108**, 7385–7390 (2011).
56. Jayasinghe, L. & Bayley, H. The leukocidin pore: evidence for an octamer with four LukF subunits and four LukS subunits alternating around a central axis. *Protein Sci.* **14**, 2550–2561 (2005).
57. Yamashita, K. *et al.* Crystal structure of the octameric pore of staphylococcal γ-hemolysin reveals the β-barrel pore formation mechanism by two components. *Proc. Natl Acad. Sci. USA* **108**, 17314–17319 (2011).
58. Song, L. *et al.* Structure of staphylococcal α-hemolysin, a heptameric transmembrane pore. *Science* **274**, 1859–1866 (1996).
This paper reported the first atomic-resolution structure of a complete PFT pore inserted in a membrane (a β-PFT pore in this case), highlighting the mechanism required for switching from a soluble inactive toxin to an active haemolytic pore.
59. Yamashita, D. *et al.* Molecular basis of transmembrane β-barrel formation of staphylococcal pore-forming toxins. *Nat. Commun.* **5**, 4897 (2014).
60. Olson, R., Nariya, H., Yokota, K., Kamio, Y. & Gouaux, E. Crystal structure of staphylococcal LukF delineates conformational changes accompanying formation of a transmembrane channel. *Nat. Struct. Biol.* **6**, 134–140 (1999).
61. Olson, R. & Gouaux, E. Crystal structure of the *Vibrio cholerae* cytolysin (VCC) pro-toxin and its assembly into a heptameric transmembrane pore. *J. Mol. Biol.* **350**, 997–1016 (2005).
62. Huyet, J. *et al.* Structural insights into δ-toxin pore formation. *PLoS ONE* **8**, e66673 (2013).
63. Paul, K. & Chattopadhyay, K. Pre-pore oligomer formation by *Vibrio cholerae* cytolysin: insights from a truncated variant lacking the pore-forming pre-stem loop. *Biochem. Biophys. Res. Commun.* **443**, 189–193 (2014).
64. Iacovache, I., Dal Peraro, M. & van der Goot, F. G. *The Comprehensive Sourcebook of Bacterial Protein Toxins* (Elsevier Ltd, 2015).
65. Ballard, J., Sokolov, Y., Yuan, W.-L., Kagan, B. L. & Tweten, R. K. Activation and mechanism of *Clostridium septicum* α-toxin. *Mol. Microbiol.* **10**, 627–634 (1993).
66. Opota, O. *et al.* Monalysin, a novel ss-pore-forming toxin from the *Drosophila* pathogen *Pseudomonas entomophila*, contributes to host intestinal damage and lethality. *PLoS Pathog.* **7**, e1002259 (2011).
67. Zhao, F. *et al.* Comprehensive transcriptome profiling and functional analysis of the frog (*Bombina maxima*) immune system. *DNA Res.* **21**,1–13 (2013).
68. Gao, Q. *et al.* βγ-CAT, a non-lens βγ-crystallin and trefoil factor complex, induces calcium-dependent platelet apoptosis. *Thromb. Haemost.* **105**, 846–854 (2011).
69. Parker, M. W. *et al.* Structure of the *Aeromonas* toxin proaerolysin in its water-soluble and membrane-channel states. *Nature* **367**, 292–295 (1994).
This paper reported the first structure of a β-PFT in its soluble form and an initial model of pore architecture based on low-resolution EM data.
70. Abrami, L., Fivaz, M. & van Der Goot, F. G. Adventures of a pore-forming toxin at the target cell surface. *Trends Microbiol.* **8**, 168–172 (2000).
71. Iacovache, I. *et al.* A rivet model for channel formation by aerolysin-like pore-forming toxins. *EMBO J.* **25**, 457–466 (2006).
72. Melton, J. A., Parker, M. W., Rossjohn, J., Buckley, J. T. & Tweten, R. K. The identification and structure of the membrane-spanning domain of the *Clostridium* septicum α-toxin. *J. Biol. Chem.* **279**, 14315–14322 (2004).
73. Howard, S. P. & Buckley, J. T. Activation of the hole forming toxin aerolysin by extracellular processing. *J. Bacteriol.* **163**, 336–340 (1985).
74. Iacovache, I. *et al.* Dual chaperone role of the C-terminal propeptide in folding and oligomerization of the pore-forming toxin aerolysin. *PLoS Pathog.* **7**, e1002135 (2011).
75. Degiacomi, M. T. *et al.* Molecular assembly of the aerolysin pore reveals a swirling membrane-insertion mechanism. *Nat. Chem. Biol.* **9**, 623–629 (2013).
This study used an integrative modelling approach to reveal the architecture of the aerolysin pore at a near-atomic resolution.
76. Unno, H., Goda, S. & Hatakeyama, T. Hemolytic lectin CEL-III heptamerizes via a large structural transition from α-helices to a β-barrel during the transmembrane pore formation process. *J. Biol. Chem.* **289**, 12805–12812 (2014).
77. Popoff, M. R. ε-toxin: a fascinating pore-forming toxin. *FEBS J.* **278**, 4602–4615 (2011).
78. Popoff, M. R. Clostridial pore-forming toxins: powerful virulence factors. *Anaerobe* **30**, 220–238 (2014).
79. Briggs, D. C. *et al.* Structure of the food-poisoning *Clostridium perfringens* enterotoxin reveals similarity to the aerolysin-like pore-forming toxins. *J. Mol. Biol.* **413**, 138–149 (2011).
80. Kitadokoro, K. *et al.* Crystal structure of *Clostridium perfringens* enterotoxin displays features of β-pore-forming toxins. *J. Biol. Chem.* **286**, 19549–19555 (2011).
81. Yelland, T. S. *et al.* Structure of a *C. perfringens* enterotoxin mutant in complex with a modified Claudin-2 extracellular loop 2. *J. Mol. Biol.* **426**, 3134–3147 (2014).
82. Mancheno, J. M., Tateno, H., Goldstein, I. J., Martinez-Ripoll, M. & Hermoso, J. A. Structural analysis of the *Laetiporus sulphureus* hemolytic pore-forming lectin in complex with sugars. *J. Biol. Chem.* **280**, 17251–17259 (2005).
83. Sher, D. J. *et al.* Hydralysins: a new category of β-pore-forming toxins in cnidaria. Characterization and preliminary structure-function analysis. *J. Biol. Chem.* **280**, 22847–22855 (2005).
84. De Colibus, L. *et al.* Structures of lysenin reveal a shared evolutionary origin for pore-forming proteins and its mode of sphingomyelin recognition. *Structure* **20**, 1498–1507 (2012).
85. Hotze, E. M. & Tweten, R. K. Membrane assembly of the cholesterol-dependent cytolysin pore complex. *Biochim. Biophys. Acta* **1818**, 1028–1038 (2012).
86. Hotze, E. M. *et al.* Identification and characterization of the first cholesterol-dependent cytolysins from Gram-negative bacteria. *Infect. Immun.* **81**, 216–225 (2013).
87. Hadders, M. A., Beringer, D. X. & Gros, P. Structure of C8α-MACPF reveals mechanism of membrane attack in complement immune defense. *Science* **317**, 1552–1554 (2007).
88. Rosado, C. J. *et al.* A common fold mediates vertebrate defense and bacterial attack. *Science* **317**, 1548–1551 (2007).
89. Law, R. H. *et al.* The structural basis for membrane binding and pore formation by lymphocyte perforin. *Nature* **468**, 447–451 (2010).
90. Lukoyanova, N. *et al.* Conformational changes during pore formation by the perforin-related protein pleurotolysin. *PLoS Biol.* **13**, e1002049 (2015).
91. Roiko, M. S. & Carruthers, V. B. New roles for perforins and proteases in apicomplexan egress. *Cell. Microbiol.* **11**, 1444–1452 (2009).
92. Deligianni, E. *et al.* A perforin-like protein mediates disruption of the erythrocyte membrane during egress of *Plasmodium berghei* male gametocytes. *Cell. Microbiol.* **15**, 1438–1455 (2013).
93. Xu, Q. *et al.* Structure of a membrane-attack complex/perforin (MACPF) family protein from the human gut symbiont *Bacteroides thetaiotaomicron*. *Acta Crystallogr. Sect. F. Struct. Biol. Cryst. Commun.* **66**, 1297–1305 (2010).
94. Chatzidaki-Livanis, M., Coyne, M. J. & Comstock, L. E. An antimicrobial protein of the gut symbiont *Bacteroides fragilis* with a MACPF domain of host immune proteins. *Mol. Microbiol.* **94**, 1361–1374 (2014).
95. Rossjohn, J., Feil, S. C., McKinstry, W. J., Tweten, R. K. & Parker, M. W. Structure of a cholesterol-binding, thiol-activated cytolysin and a model of its membrane form. *Cell* **89**, 685–692 (1997).
This paper presented the first structure of a CDC (PFO) and a model of the pore, which revealed the mechanism of pore insertion and the role of cholesterol lipids as CDC receptors.
96. Xu, L. *et al.* Crystal structure of cytotoxin protein suilysin from *Streptococcus* suis. *Protein Cell* **1**, 96–105 (2010).

97. Johnson, S., Brooks, N. J., Smith, R. A., Lea, S. M. & Bubeck, D. Structural basis for recognition of the pore-forming toxin intermedilysin by human complement receptor CD59. *Cell Rep.* **3**, 1369–1377 (2013).
98. Koster, S. *et al.* Crystal structure of listeriolysin O reveals molecular details of oligomerization and pore formation. *Nat. Commun.* **5**, 3690 (2014).
99. Feil, S. C. *et al.* Structure of the lectin regulatory domain of the cholesterol-dependent cytolysin lectinolysin reveals the basis for its lewis antigen specificity. *Structure* **20**, 248–258 (2012).
100. Bourdeau, R. W. *et al.* Cellular functions and X-ray structure of anthrolysin O, a cholesterol-dependent cytolysin secreted by *Bacillus anthracis*. *J. Biol. Chem.* **284**, 14645–14656 (2009).
101. Feil, S. C., Ascher, D. B., Kuiper, M. J., Tweten, R. K. & Parker, M. W. Structural studies of *Streptococcus pyogenes* streptolysin O provide insights into the early steps of membrane penetration. *J. Mol. Biol.* **426**, 785–792 (2014).
102. Tilley, S. J., Orlova, E. V., Gilbert, R. J., Andrew, P. W. & Saibil, H. R. Structural basis of pore formation by the bacterial toxin pneumolysin. *Cell* **121**, 247–256 (2005).
103. Czajkowsky, D. M., Hotze, E. M., Shao, Z. & Tweten, R. K. Vertical collapse of a cytolysin prepore moves its transmembrane β-hairpins to the membrane. *EMBO J.* **23**, 3206–3215 (2004).
104. Shepard, L. A. *et al.* Identification of a membrane-spanning domain of the thiol-activated pore-forming toxin *Clostridium perfringens* perfringolysin O: an α-helical to β-sheet transition identified by fluorescence spectroscopy. *Biochemistry* **37**, 14563–14574 (1998).
This study revealed a structure for the membrane-spanning domain of PFO, and showed the structural switch that accompanies pore formation.
105. Shatursky, O. *et al.* The mechanism of membrane insertion for a cholesterol-dependent cytolysin: a novel paradigm for pore-forming toxins. *Cell* **99**, 293–299 (1999).
106. Sato, T. K., Tweten, R. K. & Johnson, A. E. Disulfide-bond scanning reveals assembly state and β-strand tilt angle of the PFO β-barrel. *Nat. Chem. Biol.* **9**, 383–389 (2013).
107. Ramachandran, R., Tweten, R. K. & Johnson, A. E. Membrane-dependent conformational changes initiate cholesterol-dependent cytolysin oligomerization and intersubunit β-strand alignment. *Nat. Struct. Mol. Biol.* **11**, 697–705 (2004).
108. Sonnen, A. F., Plitzko, J. M. & Gilbert, R. J. Incomplete pneumolysin oligomers form membrane pores. *Open Biol.* **4**, 140044 (2014).
109. Leung, C. *et al.* Stepwise visualization of membrane pore formation by suilysin, a bacterial cholesterol-dependent cytolysin. *eLIFE* **3**, e04247 (2014).
110. Wade, K. R. *et al.* An intermolecular electrostatic interaction controls the prepore-to-pore transition in a cholesterol-dependent cytolysin. *Proc. Natl Acad. Sci. USA* **112**, 2204–2209 (2015).
111. Reboul, C. F., Whisstock, J. C. & Dunstone, M. A. A new model for pore formation by cholesterol-dependent cytolysins. *PLoS Comput. Biol.* **10**, e1003791 (2014).
112. Jiang, J., Pentelute, B. L., Collier, R. J. & Zhou, Z. H. Atomic structure of anthrax protective antigen pore elucidates toxin translocation. *Nature* **521**, 545–549 (2015).
113. Kintzer, A. F., Sterling, H. J., Tang, I. I., Williams, E. R. & Krantz, B. A. Anthrax toxin receptor drives protective antigen oligomerization and stabilizes the heptameric and octameric oligomer by a similar mechanism. *PLoS ONE* **5**, e13888 (2010).
114. Krantz, B. A. *et al.* A phenylalanine clamp catalyzes protein translocation through the anthrax toxin pore. *Science* **309**, 777–781 (2005).
115. Meusch, D. *et al.* Mechanism of Tc toxin action revealed in molecular detail. *Nature* **508**, 61–65 (2014).
116. Gatsogiannis, C. *et al.* A syringe-like injection mechanism in *Photorhabdus luminescens* toxins. *Nature* **495**, 520–523 (2013).
117. Levan, S., De, S. & Olson, R. *Vibrio cholerae* cytolysin recognizes the heptasaccharide core of complex N-glycans with nanomolar affinity. *J. Mol. Biol.* **425**, 944–957 (2013).
118. Rai, A. K., Paul, K. & Chattopadhyay, K. Functional mapping of the lectin activity site on the β-prism domain of *Vibrio cholerae* cytolysin: implications for the membrane pore-formation mechanism of the toxin. *J. Biol. Chem.* **288**, 1665–1673 (2013).
119. Kaus, K., Lary, J. W., Cole, J. L. & Olson, R. Glycan specificity of the *Vibrio vulnificus* hemolysin lectin outlines evolutionary history of membrane targeting by a toxin family. *J. Mol. Biol.* **426**, 2800–2812 (2014).
120. Hong, Y. *et al.* Requirement of N-glycan on GPI-anchored proteins for efficient binding of aerolysin but not *Clostridium septicum* α-toxin. *EMBO J.* **21**, 5047–5056 (2002).
121. Diep, D. B., Nelson, K. L., Raja, S. M., cMaster, R. W. & Buckley, J. T. Glycosylphosphatidylinositol anchors of membrane glycoproteins are binding determinants for the channel-forming toxin aerolysin. *J. Biol. Chem.* **273**, 2355–2360 (1998).
122. Cole, A. R. *et al. Clostridium perfringens* ε-toxin shows structural similarity to the pore-forming toxin aerolysin. *Nat. Struct. Mol. Biol.* **11**, 797–798 (2004).
123. Akiba, T. *et al.* Crystallization of parasporin-2, a *Bacillus thuringiensis* crystal protein with selective cytocidal activity against human cells. *Acta Crystallogr. D Biol. Crystallogr.* **60**, 2355–2357 (2004).
124. Ivie, S. E. & McClain, M. S. Identification of amino acids important for binding of *Clostridium perfringens* ε-toxin to host cells and to HAVCR1. *Biochemistry* **51**, 7588–7595 (2012).
125. Bokori-Brown, M. *et al. Clostridium perfringens* ε-toxin H149A mutant as a platform for receptor binding studies. *Protein Sci.* **22**, 650–659 (2013).
126. Shewell, L. K. *et al.* The cholesterol-dependent cytolysins pneumolysin and streptolysin O require binding to red blood cell glycans for hemolytic activity. *Proc. Natl Acad. Sci. USA* **111**, E5312–5320 (2014).
127. Johnson, C. L. *et al.* The antibacterial toxin colicin N binds to the inner core of lipopolysaccharide and close to its translocator protein. *Mol. Microbiol.* **92**, 440–452 (2014).
128. Mukherjee, S. *et al.* Antibacterial membrane attack by a pore-forming intestinal C-type lectin. *Nature* **505**, 103–107 (2014).
129. Fivaz, M., Abrami, L. & van der Goot, F. G. Landing on lipid rafts. *Trends Cell Biol.* **9**, 212–213 (1999).
130. Abrami, L. & van der Goot, F. G. Plasma membrane microdomains act as concentration platforms to facilitate intoxication by aerolysin. *J. Cell Biol.* **147**, 175–184 (1999).
131. Kobayashi, T., Makino, A., Ishii, K., Yamaji, A. & Kiyokawa, E. Lysenin:sphingomyelin specific probe. *Mol Biol Cell Abstr.* **11**, 314a (2000).
132. Skocaj, M. *et al.* The sensing of membrane microdomains based on pore-forming toxins. *Curr. Med. Chem.* **20**, 491–501 (2013).
133. Lin, Q. & London, E. Altering hydrophobic sequence lengths shows that hydrophobic mismatch controls affinity for ordered lipid domains (rafts) in the multitransmembrane strand protein perfringolysin O. *J. Biol. Chem.* **288**, 1340–1352 (2013).
134. Tweten, R. K. Cholesterol-dependent cytolysins, a family of versatile pore-forming toxins. *Infect. Immun.* **73**, 6199–6209 (2005).
135. Dowd, K. J., Farrand, A. J. & Tweten, R. K. The cholesterol-dependent cytolysin signature motif: a critical element in the allosteric pathway that couples membrane binding to pore assembly. *PLoS Pathog.* **8**, e1002787 (2012).
136. Farrand, A. J., LaChapelle, S., Hotze, E. M., Johnson, A. E. & Tweten, R. K. Only two amino acids are essential for cytolytic toxin recognition of cholesterol at the membrane surface. *Proc. Natl Acad. Sci. USA* **107**, 4341–4346 (2010).
137. Alonzo, F. *et al.* CCR5 is a receptor for *Staphylococcus aureus* leukotoxin ED. *Nature* **493**, 51–55 (2013).
This study revealed how the selectivity of leukocidins towards different immune cells is mediated by specific chemokine receptors.
138. Reyes-Robles, T. *et al. Staphylococcus aureus* leukotoxin ED targets the chemokine receptors CXCR1 and CXCR2 to kill leukocytes and promote infection. *Cell Host Microbe* **14**, 453–459 (2013).
S. aureus **LukED is shown in this study to target both innate and adaptive immune responses by binding to CXCR1 and CXCR2 on neutrophils in addition to its established role of binding to CCR5 on T lymphocytes, macrophages and dendritic cells.**
139. Spaan, A. N. *et al.* The staphylococcal toxin Panton-Valentine leukocidin targets human C5a receptors. *Cell Host Microbe* **13**, 584–594 (2013).
140. Spaan, A. N. *et al.* The staphylococcal toxins γ-haemolysin AB and CB differentially target phagocytes by employing specific chemokine receptors. *Nat. Commun.* **5**, 5438 (2014).
141. Wilke, G. A. & Bubeck Wardenburg, J. Role of a disintegrin and metalloprotease 10 in *Staphylococcus aureus* α-hemolysin-mediated cellular injury. *Proc. Natl Acad. Sci. USA* **107**, 13473–13478 (2010).
142. Berube, B. J. & Bubeck Wardenburg, J. *Staphylococcus aureus* α-toxin: nearly a century of intrigue. *Toxins (Basel)* **5**, 1140–1166 (2013).
143. Giddings, K. S., Zhao, J., Sims, P. J. & Tweten, R. K. Human CD59 is a receptor for the cholesterol-dependent cytolysin intermedilysin. *Nat. Struct. Mol. Biol.* **11**, 1173–1178 (2004).
This study extended the known cellular specificity of CDCs by showing that they bind to protein receptors such as CD59 in addition to cholesterol.
144. Tabata, A. *et al.* The diversity of receptor recognition in cholesterol-dependent cytolysins. *Microbiol. Immunol.* **58**, 155–171 (2014).
145. Yang, W. S. *et al.* Suicide cancer gene therapy using pore-forming toxin, streptolysin O. *Mol. Cancer Ther.* **5**, 1610–1619 (2006).
146. Ayub, M., Stoddart, D. & Bayley, H. Nucleobase recognition by truncated α-hemolysin pores. *ACS Nano* **9**, 7895–7903 (2015).
147. Stoddart, D. *et al.* Functional truncated membrane pores. *Proc. Natl Acad. Sci. USA* **111**, 2425–2430 (2014).
148. Dong, J. *et al.* Oroxylin A inhibits hemolysis via hindering the self-assembly of α-hemolysin heptameric transmembrane pore. *PLoS Comput. Biol.* **9**, e1002869 (2013).
149. Qiu, J. *et al.* Molecular modeling reveals the novel inhibition mechanism and binding mode of three natural compounds to staphylococcal α-hemolysin. *PLoS ONE* **8**, e80197 (2013).
150. Vivekananda, J., Salgado, C. & Millenbaugh, N. J. DNA aptamers as a novel approach to neutralize *Staphylococcus aureus* α-toxin. *Biochem. Biophys. Res. Commun.* **444**, 433–438 (2014).
151. Rai, A. K. & Chattopadhyay, K. Trapping of *Vibrio cholerae* cytolysin in the membrane-bound monomeric state blocks membrane insertion and functional pore formation by the toxin. *J. Biol. Chem.* **289**, 16978–16987 (2014).
152. Wu, Q. & Guo, Z. Glycosylphosphatidylinositols are potential targets for the development of novel inhibitors for aerolysin-type of pore-forming bacterial toxins. *Med. Res. Rev.* **30**, 258–269 (2010).
153. Foletti, D. *et al.* Mechanism of action and *in vivo* efficacy of a human-derived antibody against *Staphylococcus aureus* α-hemolysin. *J. Mol. Biol.* **425**, 1641–1654 (2013).
154. Inoshima, I. *et al.* A *Staphylococcus aureus* pore-forming toxin subverts the activity of ADAM10 to cause lethal infection in mice. *Nat. Med.* **17**, 1310–1314 (2011).
155. Fernandes da Costa, S. P. *et al.* Identification of a key residue for oligomerisation and pore-formation of *Clostridium perfringens* NetB. *Toxins (Basel)* **6**, 1049–1061 (2014).
156. Bokori-Brown, M. *et al. Clostridium perfringens* ε toxin mutant Y30A-Y196A as a recombinant vaccine candidate against enterotoxemia. *Vaccine* **32**, 2682–2687 (2014).
157. Cockeran, R. *et al.* Characterization of the interactions of the pneumolysoid, Δ6 PLY, with human neutrophils *in vitro*. *Vaccine* **29**, 8780–8782 (2011).
158. Douce, G., Ross, K., Cowan, G., Ma, J. T. & Mitchell, T. J. Novel mucosal vaccines generated by genetic conjugation of heterologous proteins to pneumolysin (PLY) from *Streptococcus pneumoniae*. *Vaccine* **28**, 3231–3237 (2010).
159. Mann, B. *et al.* Broadly protective protein-based pneumococcal vaccine composed of pneumolysin toxoid-CbpA peptide recombinant fusion protein. *J. Infect. Dis.* **209**, 1116–1125 (2014).
160. Hu, C. M. & Zhang, L. Nanotoxoid vaccines. *Nano Today* **9**, 401–404 (2014).
161. Hu, C. M., Fang, R. H., Luk, B. T. & Zhang, L. Nanoparticle-detained toxins for safe and effective vaccination. *Nat. Nanotechnol.* **8**, 933–938 (2013).
This study used Hla pores embedded in membrane-coated nanoparticles to promote an enhanced toxin-specific immune response.
162. Walther, W. *et al.* Novel *Clostridium perfringens* enterotoxin suicide gene therapy for selective treatment of claudin-3- and -4-overexpressing tumors. *Gene Ther.* **19**, 494–503 (2012).

163. Lal-Nag, M., Battis, M., Santin, A. D. & Morin, P. J. Claudin-6: a novel receptor for CPE-mediated cytotoxicity in ovarian cancer. *Oncogenesis* **1**, e33 (2012).
164. Veshnyakova, A. *et al.* Mechanism of *Clostridium perfringens* enterotoxin interaction with Claudin-3/-4 protein suggests structural modifications of the toxin to target specific claudins. *J. Biol. Chem.* **287**, 1698–1708 (2012).
165. Linhartova, I. *et al.* RTX proteins: a highly diverse family secreted by a common mechanism. *FEMS Microbiol. Rev.* **34**, 1076–1112 (2010).
166. Kudryashova, E., Heisler, D., Zywiec, A. & Kudryashov, D. S. Thermodynamic properties of the effector domains of MARTX toxins suggest their unfolding for translocation across the host membrane. *Mol. Microbiol.* **92**, 1056–1071 (2014).
167. Hyland, C., Vuillard, L., Hughes, C. & Koronakis, V. Membrane interaction of *Escherichia coli* hemolysin: flotation and insertion-dependent labeling by phospholipid vesicles. *J. Bacteriol.* **183**, 5364–5370 (2001).
168. Gonzalez, M. R. *et al.* Pore-forming toxins induce multiple cellular responses promoting survival. *Cell. Microbiol.* **13**, 1026–1043 (2011).
169. Gurcel, L., Abrami, L., Girardin, S., Tschopp, J. & van der Goot, F. G. Caspase-1 activation of lipid metabolic pathways in response to bacterial pore-forming toxins promotes cell survival. *Cell* **126**, 1135–1145 (2006).
170. Higa, N. *et al. Vibrio parahaemolyticus* effector proteins suppress inflammasome activation by interfering with host autophagy signaling. *PLoS Pathog.* **9**, e1003142 (2013).
171. Nagahama, M. *et al.* The p38 MAPK and JNK pathways protect host cells against *Clostridium perfringens* β-toxin. *Infect. Immun.* **81**, 3703–3708 (2013).
172. Craven, R. R. *et al. Staphylococcus aureus* α-hemolysin activates the NLRP3-inflammasome in human and mouse monocytic cells. *PLoS ONE* **4**, e7446 (2009).
173. Soong, G., Chun, J., Parker, D. & Prince, A. *S. aureus* activation of caspase-1/calpain signaling mediates invasion through human keratinocytes. *J. Infect. Dis.* **205**, 1571–1579 (2012).
174. Holzinger, D. *et al. Staphylococcus aureus* Panton-Valentine leukocidin induces an inflammatory response in human phagocytes via the NLRP3 inflammasome. *J. Leukoc. Biol.* **92**, 1069–1081 (2012).
175. Di Venanzio, G., Stepanenko, T. M. & Garcia Vescovi, E. *Serratia marcescens* ShlA pore-forming toxin is responsible for early induction of autophagy in host cells and is transcriptionally regulated by RcsB. *Infect. Immun.* **82**, 3542–3554 (2014).
176. Mestre, M. B. & Colombo, M. I. Autophagy and toxins: a matter of life or death. *Curr. Mol. Med.* **13**, 241–251 (2013).
177. Mestre, M. B. & Colombo, M. I. *Staphylococcus aureus* promotes autophagy by decreasing intracellular cAMP levels. *Autophagy* **8**, 1865–1867 (2012).
178. Hamon, M. A. *et al.* Histone modifications induced by a family of bacterial toxins. *Proc. Natl Acad. Sci. USA* **104**, 13467–13472 (2007).
179. Walev, I. *et al.* Delivery of proteins into living cells by reversible membrane permeabilization with streptolysin-O. *Proc. Natl Acad. Sci. USA* **98**, 3185–3190 (2001).
180. Keefe, D. *et al.* Perforin triggers a plasma membrane-repair response that facilitates CTL induction of apoptosis. *Immunity* **23**, 249–262 (2005).
181. McNeil, P. L. & Kirchhausen, T. An emergency response team for membrane repair. *Nat. Rev. Mol. Cell Biol.* **6**, 499–505 (2005).
182. Lesieur, C. *et al.* Increased stability upon heptamerization of the pore-forming toxin aerolysin. *J. Biol. Chem.* **274**, 36722–36728 (1999).
183. Idone, V., Tam, C. & Andrews, N. W. Two-way traffic on the road to plasma membrane repair. *Trends Cell Biol.* **18**, 552–559 (2008).
184. Husmann, M. *et al.* Elimination of a bacterial pore-forming toxin by sequential endocytosis and exocytosis. *FEBS Lett.* **583**, 337–344 (2009).
185. Corrotte, M. *et al.* Caveolae internalization repairs wounded cells and muscle fibers. *eLIFE* **2**, e00926 (2013).
186. Keyel, P. A. *et al.* Streptolysin O clearance through sequestration into blebs that bud passively from the plasma membrane. *J. Cell Sci.* **124**, 2414–2423 (2011).
187. Jimenez, A. J. *et al.* ESCRT machinery is required for plasma membrane repair. *Science* **343**, 1247136 (2014).
188. Henne, W. M., Buchkovich, N. J. & Emr, S. D. The ESCRT pathway. *Dev. Cell* **21**, 77–91 (2011).
189. Strack, B., Calistri, A., Craig, S., Popova, E. & Gottlinger, H. G. AIP1/ALIX is a binding partner for HIV-1 p6 and EIAV p9 functioning in virus budding. *Cell* **114**, 689–699 (2003).
190. Prescher, J. *et al.* Super-resolution imaging of ESCRT-proteins at HIV-1 assembly sites. *PLoS Pathog.* **11**, e1004677 (2015).
191. Degiacomi, M. T. & Dal Peraro, M. Macromolecular symmetric assembly prediction using swarm intelligence dynamic modeling. *Structure* **21**, 1097–1106 (2013).
192. Tamo, G. E., Abriata, L. A. & Dal Peraro, M. The importance of dynamics in integrative modeling of supramolecular assemblies. *Curr. Opin. Struct. Biol.* **31**, 28–34 (2015).
193. Spiga, E., Degiacomi, M. T. & Dal Peraro, M. New strategies for integrative dynamic modeling of macromolecular assembly. *Adv. Protein Chem. Struct. Biol.* **96**, 77–111 (2014).
194. Russel, D. *et al.* Putting the pieces together: integrative modeling platform software for structure determination of macromolecular assemblies. *PLoS Biol.* **10**, e1001244 (2012).
195. Thalassinos, K., Pandurangan, A. P., Xu, M., Alber, F. & Topf, M. Conformational states of macromolecular assemblies explored by integrative structure calculation. *Structure* **21**, 1500–1508 (2013).
196. Kudryashev, M. *et al. In situ* structural analysis of the *Yersinia enterocolitica* injectisome. *eLIFE* **2**, e00792 (2013).
197. Sali, A. *et al.* Outcome of the first wwPDB hybrid/integrative methods task force workshop. *Structure* **23**, 1156–1167 (2015).
198. Leone, P. *et al.* X-ray and cryo-electron microscopy structures of monalysin pore-forming toxin reveal multimerization of the pro-form. *J. Biol. Chem.* **290**, 13191–13201 (2015).

Acknowledgements
Work in the authors' laboratories is supported by the Swiss National Science Foundation (SNSF). The authors apologize to colleagues whose work could not be duly discussed owing to space limitations. The authors thank M. Dunstone for providing the coordinates of perfringolysin O oligomers used in the figures.

Competing interests statement
The authors declare no competing interests.

DATABASES
RCSB Protein Data Bank:
http://www.rcsb.org/pdb/home/home.do
1COL | 1QOY | 2WCD | 4TSL | 4TSN | 4TSY | 4IDJ | 7AHL | 4P1Y | 1PRE | 1PFO

ALL LINKS ARE ACTIVE IN THE ONLINE PDF